(43, 44). Dysfunction of other cell lineage may also be indirectly involved in impaired osteoblast function *in vivo*. For example, the defective production of osteonectin and biglycan in bone marrow macrophages, as shown in our gene expression analysis (supplemental Table 2), might damage osteoblast functions in the DKO mice as described previously (45, 46).

Cigarette smoking is known as a common risk factor for COPD and osteoporosis, which are both characterized by net loss of lung or bone tissue mass (47), and the phenotype of DKO mice has raised a possibility that these two pathological conditions might share common mechanisms involving tetraspanins. Further studies using human samples are needed because there are considerable differences in physiology and anatomy between mice and humans (48).

In conclusion, this study has shown that tetraspanins CD9 and CD81, which regulate motility and MMP production of macrophages, are down-regulated by smoking-related pro-inflammatory stimuli. Double deficiency of these tetraspanins causes age-related progression of pulmonary emphysema and osteopenia in mice. Given that tetraspanins function as molecular facilitator, the loss of CD9 and CD81 could lead to disordered organization of molecules that otherwise associate with these tetraspanins. Such defective molecular organization might be a part of mechanisms underlying the lung disease and osteoporosis in human COPD.

Acknowledgments—We thank T. Miyazaki (University of Texas Southwestern Medical Center, Dallas) for providing CD81 KO mice; M. Kobayashi (Osaka University) for assistance in mouse genotyping; Y. Tomita and S. Furue (Shionogi and Co., Ltd., Osaka, Japan) for assistance in chord length measurement; T. Yoneda (Osaka University Graduate School of Dentistry, Osaka, Japan) for helpful comments on bone analysis; T. Ito and K. Ozawa (Osaka University Graduate School of Medicine) for helpful comments on kidney and skin histology, respectively; Y. Satou (Teijin Pharma Ltd.) and M. Hamaoka (Osaka University) for technical assistance; and Y. Habe for secretarial assistance.

REFERENCES

1. Shapiro, S. D. (2002) *Biochem. Soc. Trans.* **30,** 98–102
2. Barnes, P. J., Shapiro, S. D., and Pauwels, R. A. (2003) *Eur. Respir. J.* **22,** 672–688
3. Finlay, G. A., O'Driscoll, L. R., Russell, K. J., D'Arcy, E. M., Masterson, J. B., FitzGerald, M. X., and O'Connor, C. M. (1997) *Am. J. Respir. Crit. Care Med.* **156,** 240–247
4. Ohnishi, K., Takagi, M., Kurokawa, Y., Satomi, S., and Konttinen, Y. T. (1998) *Lab. Investig.* **78,** 1077–1087
5. Barnes, P. J. (2006) *Chest* **129,** 151–155
6. Hemler, M. E. (2005) *Nat. Rev. Mol. Cell Biol.* **6,** 801–811
7. Sugiura, T., and Berditchevski, F. (1999) *J. Cell Biol.* **146,** 1375–1389
8. Saito, Y., Tachibana, I., Takeda, Y., Yamane, H., He, P., Suzuki, M., Minami, S., Kijima, T., Yoshida, M., Kumagai, T., Osaki, T., and Kawase, I. (2006) *Cancer Res.* **66,** 9557–9565
9. Tohami, T., Drucker, L., Shapiro, H., Radnay, J., and Lishner, M. (2007) *FASEB J.* **21,** 691–699
10. Hoshino, S., Yoshida, M., Inoue, K., Yano, Y., Yanagita, M., Mawatari, H., Yamane, H., Kijima, T., Kumagai, T., Osaki, T., Tachiba, I., and Kawase, I. (2005) *Biochem. Biophys. Res. Commun.* **329,** 58–63
11. Shibata, Y., Zsengeller, Z., Otake, K., Palaniyar, N., and Trapnell, B. C. (2001) *Blood* **98,** 2845–2852
12. Wang, Z., Zheng, T., Zhu, Z., Homer, R. J., Riese, R. J., Chapman, H. A., Jr., Shapiro, S. D., and Elias, J. A. (2000) *J. Exp. Med.* **192,** 1587–1600
13. Takeda, Y., Tachibana, I., Miyado, K., Kobayashi, M., Miyazaki, T., Funakoshi, T., Kimura, H., Yamane, H., Saito, Y., Goto, H., Yoneda, T., Yoshida, M., Kumagai, T., Osaki, T., Hayashi, S., Kawase, I., and Mekada, E. (2003) *J. Cell Biol.* **161,** 945–956
14. Zheng, T., Zhu, Z., Wang, Z., Homer, R. J., Ma, B., Riese, R. J., Jr., Chapman, H. A., Jr., Shapiro, S. D., and Elias, J. A. (2000) *J. Clin. Investig.* **106,** 1081–1093
15. Liu, W., Toyosawa, S., Furuichi, T., Kanatani, N., Yoshida, C., Liu, Y., Himeno, M., Narai, S., Yamaguchi, A., and Komori, T. (2001) *J. Cell Biol.* **155,** 157–166
16. Lind, P. M., Lind, L., Larsson, S., and Orberg, J. (2001) *Bone (Elmsford)* **29,** 265–270
17. Ito, K., Lim, S., Caramori, G., Cosio, B., Chung, K. F., Adcock, I. M., and Barnes, P. J. (2002) *Proc. Natl. Acad. Sci. U. S. A.* **99,** 8921–8926
18. Park, G. Y., Park, J. W., Jeong, D. H., and Jeong, S. H. (2003) *Chest* **123,** 475–480
19. Cawston, T., Carrere, S., Catterall, J., Duggleby, R., Elliott, S., Shingleton, B., and Rowan, A. (2001) *Novartis Found. Symp.* **234,** 205–228
20. Ogawa, K., Chen, F., Kuang, C., and Chen, Y. (2004) *Biochem. J.* **381,** 413–422
21. Hemler, M. E. (2003) *Annu. Rev. Cell Dev. Biol.* **19,** 397–422
22. Finlay, G. A., O'Donnell, M. D., O'Connor, C. M., Hayes, J. P., and FitzGerald, M. X. (1996) *Am. J. Pathol.* **149,** 1405–1415
23. Jeffery, P. K. (2001) *Am. J. Respir. Crit. Care Med.* **164,** S28–S38
24. Lucattelli, M., Cavarra, E., de Santi, M. M., Tetley, T. D., Martorana, P. A., and Lungarella, G. (2003) *Eur. Respir. J.* **22,** 728–734
25. Kasahara, Y., Tuder, R. M., Cool, C. D., Lynch, D. A., Flores, S. C., and Voelkel, N. F. (2001) *Am. J. Respir. Crit. Care Med.* **163,** 737–744
26. Takeda, Y., Kazarov, A. R., Butterfield, C. E., Hopkins, B. D., Benjamin, L. E., Kaipainen, A., and Hemler, M. E. (2007) *Blood* **109,** 1524–1532
27. Wang, X., Inoue, S., Gu, J., Miyoshi, E., Noda, K., Li, W., Mizuno-Horikawa, Y., Nakano, M., Asahi, M., Takahashi, M., Uozumi, N., Ihara, S., Lee, S. H., Ikeda, Y., Yamaguchi, Y., Aze, Y., Tomiyama, Y., Fujii, J., Suzuki, K., Kondo, A., Shapiro, S. D., Lopez-Otin, C., Kuwaki, T., Okabe, M., Honke, K., and Taniguchi, N. (2005) *Proc. Natl. Acad. Sci. U. S. A.* **102,** 15791–15796
28. Nabeshima, Y. (2002) *Ageing Res. Rev.* **1,** 627–638
29. Chirco, R., Liu, X. W., Jung, K. K., and Kim, H. R. (2006) *Cancer Metastasis Rev.* **25,** 99–113
30. Nishio, M., Watanabe, K., Sasaki, J., Taya, C., Takasuga, S., Iizuka, R., Balla, T., Yamazaki, M., Watanabe, H., Itoh, R., Kuroda, S., Horie, Y., Forster, I., Mak, T. W., Yonekawa, H., Penninger, J. M., Kanaho, Y., Suzuki, A., and Sasaki, T. (2007) *Nat. Cell Biol.* **9,** 36–44
31. Greenlee, K. J., Werb, Z., and Kheradmand, F. (2007) *Physiol. Rev.* **87,** 69–98
32. Miyado, K., Yamada, G., Yamada, S., Hasuwa, H., Nakamura, Y., Ryu, F., Suzuki, K., Kosai, K., Inoue, K., Ogura, A., Okabe, M., and Mekada, E. (2000) *Science* **287,** 321–324
33. Rubinstein, E., Ziyyat, A., Prenant, M., Wrobel, E., Wolf, J. P., Levy, S., Le Naour, F., and Boucheix, C. (2006) *Dev. Biol.* **290,** 351–358
34. Maecker, H. T., and Levy, S. (1997) *J. Exp. Med.* **185,** 1505–1510
35. Miyazaki, T., Muller, U., and Campbell, K. S. (1997) *EMBO J.* **16,** 4217–4225
36. Wright, J. L., and Churg, A. (2002) *Chest* **122,** S301–S306
37. Amy, R. W., Bowes, D., Burri, P. H., Haines, J., and Thurlbeck, W. M. (1977) *J. Anat.* **124,** 131–151
38. Gross, N. J. (2001) *Curr. Opin. Pulm. Med.* **7,** 84–92
39. Agusti, A. (2007) *Proc. Am. Thorac. Soc.* **4,** 522–525
40. Manolagas, S. C., and Jilka, R. L. (1995) *N. Engl. J. Med.* **332,** 305–311
41. Tuder, R. M., Yoshida, T., Arap, W., Pasqualini, R., and Petrache, I. (2006) *Proc. Am. Thorac. Soc.* **3,** 503–510
42. Inoue, K., Mikuni-Takagaki, Y., Oikawa, K., Itoh, T., Inada, M., Noguchi, T., Park, J. S., Onodera, T., Krane, S. M., Noda, M., and Itohara, S. (2006) *J. Biol. Chem.* **281,** 33814–33824
43. Ortega, N., Behonick, D., Stickens, D., and Werb, Z. (2003) *Ann. N. Y. Acad. Sci.* **995,** 109–116

44. Hadjidakis, D. J., and Androulakis, I. I. (2006) *Ann. N. Y. Acad. Sci.* **1092,** 385–396
45. Xu, T., Bianco, P., Fisher, L. W., Longenecker, G., Smith, E., Goldstein, S., Bonadio, J., Boskey, A., Heegaard, A. M., Sommer, B., Satomura, K., Dominguez, P., Zhao, C., Kulkarni, A. B., Robey, P. G., and Young, M. F. (1998) *Nat. Genet.* **20,** 78–82
46. Delany, A. M., Amling, M., Priemel, M., Howe, C., Baron, R., and Canalis, E. (2000) *J. Clin. Investig.* **105,** 915–923
47. Agusti, A. G., Noguera, A., Sauleda, J., Sala, E., Pons, J., and Busquets, X. (2003) *Eur. Respir. J.* **21,** 347–360
48. Brusselle, G. G., Bracke, K. R., Maes, T., D'Hulst, A. I., Moerloose, K. B., Joos, G. F., and Pauwels, R. A. (2006) *Pulm. Pharmacol. Ther.* **19,** 155–165

The Journal of Immunology

Tetraspanin CD9 Negatively Regulates Lipopolysaccharide-Induced Macrophage Activation and Lung Inflammation

Mayumi Suzuki, Isao Tachibana, Yoshito Takeda, Ping He, Seigo Minami, Takeo Iwasaki, Hiroshi Kida, Sho Goya, Takashi Kijima, Mitsuhiro Yoshida, Toru Kumagai, Tadashi Osaki and Ichiro Kawase

J. Immunol. 2009;182;6485-6493
doi:10.4049/jimmunol.0802797
http://www.jimmunol.org/cgi/content/full/182/10/6485

The Journal of Immunology is published twice each month by The American Association of Immunologists, Inc., 9650 Rockville Pike, Bethesda, MD 20814-3994.

Print ISSN: 0022-1767 Online ISSN: 1550-6606.

Tetraspanin CD9 Negatively Regulates Lipopolysaccharide-Induced Macrophage Activation and Lung Inflammation[1]

Mayumi Suzuki,* Isao Tachibana,[2]* Yoshito Takeda,* Ping He,*† Seigo Minami,* Takeo Iwasaki,* Hiroshi Kida,* Sho Goya,* Takashi Kijima,* Mitsuhiro Yoshida,* Toru Kumagai,* Tadashi Osaki,* and Ichiro Kawase*

Tetraspanins facilitate the formation of multiple molecular complexes at specialized membrane microdomains and regulate cell activation and motility. In the present study, the role of tetraspanin CD9 in LPS-induced macrophage activation and lung inflammation was investigated in vitro and in vivo. When CD9 function was ablated with mAb treatment, small interfering RNA transfection, or gene knockout in RAW264.7 cells or bone marrow-derived macrophages, these macrophages produced larger amounts of TNF-α, matrix metalloproteinase-2, and -9 upon stimulation with LPS in vitro, when compared with control cells. Sucrose gradient analysis revealed that CD9 partly colocalized with the LPS-induced signaling mediator, CD14, at low-density light membrane fractions. In CD9 knockout macrophages, CD14 expression, CD14 and TLR4 localization into the lipid raft, and their complex formation were increased whereas IκBα expression was decreased when compared with wild-type cells, suggesting that CD9 prevents the formation of LPS receptor complex. Finally, deletion of CD9 in mice enhanced macrophage infiltration and TNF-α production in the lung after intranasal administration of LPS in vivo, when compared with wild-type mice. These results suggest that macrophage CD9 negatively regulates LPS response at lipid-enriched membrane microdomains. *The Journal of Immunology,* **2009, 182: 6485–6493.**

Lung inflammation, which is characterized by the infiltration of inflammatory cells including alveolar macrophages and their production of proinflammatory mediators such as cytokines, oxidants, and proteinases, underlies the pathophysiology of many respiratory diseases such as acute lung injury, interstitial pneumonia, granulomatous lung disease, and pulmonary emphysema. LPS, a major component of the Gram-negative bacteria cell wall, is a potent inducer of lung inflammation (1). It stimulates macrophages to produce cytokines and increase the expression of cell adhesion molecules. LPS binding up-regulates the expression of its receptor, CD14, and recruits CD14 and TLR4 into cholesterol and sphingolipid-enriched membrane microdomains designated the lipid raft, where clustering of the CD14/TLR4 receptor complex activates MAPK and NF-κB pathways and leads to rearrangement of actin cytoskeleton (2–5). Although signaling molecules essential for LPS-induced macrophage activation have been well characterized (1), factors modifying the level of LPS-induced lung inflammation still remain to be studied. Search for such factors might help to elucidate the pathogenesis of respiratory diseases involving lung inflammation.

Tetraspanin is a protein family comprising at least 33 members such as CD9, CD63, CD81, CD82, and CD151 in mammals. Its structure spanning the membrane four times endows this protein with a propensity to associate with each other, other tetraspanin members, and functional proteins such as integrins, growth factors, human leukocyte Ags, and intracellular signaling molecules (6). At specialized membrane microdomains, designated tetraspanin-enriched microdomain (TEM)[3], tetraspanins facilitate the formation of these multimolecular complexes and thereby regulate cell activation, fusion, motility, and signaling (7). Although proteins at both rafts and TEMs can distribute into low-density light membrane fractions in sucrose gradient analysis, these microdomains are thought to be distinct in view of several aspects (8). However, recent studies have suggested that there may be an overlapping or an interaction between raft and TEM proteins. Upon stimulation of macrophages with RANKL, CD9 was localized into the lipid raft (9). Also, it was proposed that TEMs and lipid rafts may associate under certain conditions, resulting in the close proximity of a distinct set of signaling molecules in platelets (10).

We recently reported that, in mice doubly deficient in tetraspanins CD9 and CD81, macrophages infiltrated into the lung and pulmonary emphysema spontaneously developed (11, 12). This observation was not obvious in mice lacking CD9 or CD81 alone (12) and thus suggests that these tetraspanins coordinately prevent lung inflammation. However, its detailed mechanisms have yet to be clarified, and whether the loss of CD9 or CD81 alone can cause the lung inflammation under certain conditions still remains unknown. In the present study, we show that, after stimulation with LPS, the loss of CD9 function enhances macrophage activation in

*Department of Respiratory Medicine, Allergy and Rheumatic Diseases, Osaka University Graduate School of Medicine, Osaka, Japan; and †Department of Respiratory Medicine, the Second Affiliated Hospital, School of Medicine, Xi'an Jiaotong University, Xi'an, People's Republic of China

Received for publication August 29, 2008. Accepted for publication March 13, 2009.

The costs of publication of this article were defrayed in part by the payment of page charges. This article must therefore be hereby marked *advertisement* in accordance with 18 U.S.C. Section 1734 solely to indicate this fact.

[1] This work was supported by a Grant-in-Aid for Scientific Research from the Ministry of Education, Culture, Sports, Science and Technology, Japan, and a grant from Kansai Biomedical Cluster project in Saito, which is promoted by the Knowledge Cluster Initiative of the Ministry of Education, Culture, Sports, Science and Technology, Japan.

[2] Address correspondence and reprint requests to Dr. Isao Tachibana, Department of Respiratory Medicine, Allergy and Rheumatic Diseases, Osaka University Graduate School of Medicine, Osaka, Japan. E-mail address: itachi02@imed3.med.osaka-u.ac.jp

[3] Abbreviations used in this paper: TEM, tetraspanin-enriched microdomain; SIRPα, signal regulatory protein α; 2OHpβCD, 2-hydroxypropyl-β-cyclodextrin; KO, knockout; BMDM, bone marrow-derived macrophage; WT, wild type; BALF, bronchoalveolar lavage fluid; siRNA, small interfering RNA; MMP, matrix metalloproteinase.

www.jimmunol.org/cgi/doi/10.4049/jimmunol.0802797

vitro and exacerbates lung inflammation in vivo. We also propose mechanisms by which CD9 negatively regulates LPS-induced signaling. CD9 prevents CD14-dependent receptor assembly at lipid-enriched membrane microdomains.

Materials and Methods

Abs and reagents

Rat anti-mouse CD9 mAb (KMC8) and hamster anti-mouse CD81 mAb (Eat2) were purchased from BD Biosciences and U.K.-Serotec, respectively. Rat anti-CD14 mAb (rmC5–3) and goat biotinylated anti-CD14 polyclonal Ab (BAF9892) were purchased from BD Biosciences and R&D Systems, respectively. Rat anti-TLR4/MD2 complex mAb (MTS510) and rabbit anti-TLR4 polyclonal Ab (IMG577) were obtained from BioLegend and IMGENEX, respectively. Mouse anti-flotillin-1 mAb (clone 18) and goat anti-CD45 polyclonal Ab were purchased from BD Biosciences and R&D Systems, respectively. Rabbit anti-IκBα polyclonal Ab (9242) and anti-phosphorylated p38 polyclonal Ab (9211) were both from Cell Signaling Technology. Rabbit anti-p38 polyclonal Ab (sc-7149) and rabbit anti-SHP-1 polyclonal Ab (sc-287) were both obtained from Santa Cruz Biotechnology. Mouse anti-phosphotyrosine mAb (PY-20) and rabbit anti-signal regulatory protein α (SIRPα) polyclonal Ab (06–729) were purchased from BD Biosciences and Upstate Biotechnology, respectively. Phenol-extracted LPS from *Escherichia coli* O55:B5 was purchased from Sigma-Aldrich. HRP-conjugated cholera toxin B subunit was purchased from List Biological Laboratories. 2-hydroxypropyl-β-cyclodextrin (2OHpβCD) and an inhibitor of IκB kinase, BMS345541, were obtained from Nacalai Tesque and Sigma-Aldrich, respectively. Cholesterol and methyl-β-cyclodextrin were both purchased from Sigma-Aldrich.

Mice

CD9 knockout (KO) mice were provided by Dr. E. Mekada (Research Institute for Microbial Diseases, Osaka University, Osaka, Japan) (13). These mice were backcrossed >6 generations into the C57BL/6J background. The mice were bred in a barrier facility, and all animal procedures were performed in accordance with the Osaka University guidelines on animal care. Nine- to 12-wk-old CD9 KO mice and wild-type (WT) littermates matched for age and sex were used in all experiments.

Cell culture and stimulation with LPS

A mouse macrophage line, RAW264.7, was cultured in DMEM containing 10% heat-inactivated FBS, 100 U/ml penicillin, and 100 μg/ml streptomycin. Mouse bone marrow-derived macrophages (BMDMs) were prepared as previously described (14). In brief, cells were isolated by flushing the bone marrow of tibias and femurs and cultured in DMEM supplemented with 20% FBS and 30% L929 supernatant containing macrophage-stimulating factor. After 6 days of culture, adherent macrophages were detached and resuspended in DMEM supplemented with 10% FBS, 100 U/ml penicillin, and 100 μg/ml streptomycin. Mouse alveolar macrophages were obtained by bronchoalveolar lavage. Lungs of mice were subjected to lavage twice with 0.75 ml PBS. Collected cells consisting >95% of macrophages were cultured in RPMI 1640 containing 2% FBS. For stimulation with LPS, RAW264.7 cells (0.25×10^6/ml), BMDMs (0.5×10^6/ml), or alveolar macrophages (1.5×10^5/ml) were serum-starved overnight and then stimulated by adding 0.1, 1, or 0.1 μg/ml LPS, respectively. In some experiments, cells were stimulated with LPS in the presence of 10 μg/ml mAbs or 1 μM BMS345541, or cells were pretreated before LPS stimulation to deplete cholesterol with 10 mM 2OHpβCD for 30 min at 37°C. For cholesterol reloading, cells were treated with 10 mM 2OHpβCD, washed, and incubated with 80 μg/ml cholesterol and 1.5 mM methyl-β-cyclodextrin for 30 min at 37°C before LPS stimulation (15).

Immunoblotting and immunoprecipitation

Cells were lysed in lysis buffer containing 0.5% Nonidet P-40, 20 mM Tris-HCl (pH 7.4), 150 mM NaCl, 2 mM EDTA, 2 mM PMSF, 10 μg/ml aprotinin, 10 μg/ml leupeptin, 1 mM orthovanadate, and 50 mM NaF. Cell lysates containing an equal amount of protein were electrophoresed on SDS-PAGE under nonreducing conditions for CD9, CD81, CD14, CD45, TLR4, and flotillin-1 or under reducing conditions for p38, phosphorylated p38, SHP-1, and SIRPα, and transferred to Immobilon-P membranes (Millipore). The membranes were probed with primary Abs followed by peroxidase-conjugated secondary Abs. Immunoreactive bands were visualized using Western Lightning Chemiluminescent Reagent (PerkinElmer). In densitometry, blots were analyzed on a FluorChem (Alpha Innotech) using the AlphaEase software. For immunoprecipitation, cell lysates containing 500 μg protein were incubated with 1 μg of specific Abs, and then immune complexes were collected with protein G-Sepharose (Amersham Biosciences) and subjected to SDS-PAGE followed by immunoblotting.

Small interfering RNA (siRNA) transfecion

siRNA duplexes targeting mouse CD9 (SMF27B-0251) were synthesized by and purchased from B-Bridge international. RAW264.7 cells (2.5×10^5/ml) cultured in a 6-well plate were transfected with either 40 nM mixture of the siRNAs or control random RNAs (S30C-0126; B-Bridge International) using LipofectAMINE 2000 reagent (Invitrogen). The cells were cultured for 3 days and gene-silencing effect was assessed by immunobotting with anti-CD9 mAb. In some experiments, the cells were stimulated with 0.1 μg/ml LPS after 2 days of transfection.

Gelatin zymography

Samples containing equal amounts of protein from culture supernatants or bronchoalveolar lavage fluid (BALF) were electrophoresed on a 10% polyacrylamide gel containing 0.1% gelatin (Invitrogen). The gels were washed with 2.5% Triton X-100 and incubated at 37°C overnight in Novex zymogram developing buffer (Invitrogen). Gelatinolytic bands were visualized by staining with 0.1% Coomassie brilliant blue R250. The intensity of the lytic bands was quantified with the FluorChem.

RT-PCR

Total RNA was extracted with Isogen (Nippon Gene), and 1 μg RNA was subjected to RT-PCR amplification using the following oligonucleotide primers: 5′-CCACGCTGTGGTGTCCCAGACGTG-3′ and 5′-GAACTC GTGCGCTGCCACCAGGAA-3′ for matrix metalloproteinase (MMP)-2 (16); 5′-TTGAGTCCGGCAGACAATCCTTGC-3′ and 5′-CCTTATCC ACGCGAATGACGCTCT-3′ for MMP-9 (16). The thermal cycling variables were 30 cycles of 30 s at 94°C, 30 s at 60°C, and 60 s at 72°C. We confirmed that these variables yielded the amplification of template DNAs within a linear range.

Sucrose gradients

BMDMs were lysed in 500 μl of MES buffer (150 mM NaCl and 20 mM MES (pH 6.5)) supplemented with 1% Triton X-100, 2 mM PMSF, 10 μg/ml aprotinin, and 10 μg/ml leupeptin for 1 h on ice. Lysates were then sheared by successive passage through hypodermic needles (5 × 18G1 1/2, 10 × 26G1/2). The lysate was mixed with an equal volume of 90% sucrose in MES buffer, placed at the bottom of a centrifuge tube, overlaid with 4.5 ml of 30% sucrose and 3.5 ml of 5% sucrose in MES buffer. After centrifugation at 100,000 × g for 16.5 h at 4°C in a Beckman SW40Ti rotor, fractions of 1 ml each were collected from the top of the gradient. Each fraction was added with 60 μM n-octylglucoside and analyzed by SDS-PAGE using 5–20% gradient gels (Wako Pure Chemical). Protein distribution in the fractions was visualized by immunoblotting with anti-CD14 (rmC5–3), anti-TLR4 (IMG577), anti-CD9, anti-CD81, anti-CD45, and anti-flotillin-1 Abs. GM1 ganglioside was detected with HRP-conjugated cholera toxin by dot blot using equal amounts of each fraction. The density of blots was quantified with the FluorChem. In some experiments, low-density, lipid-enriched, light membrane fractions (fractions 4 and 5) or dense fractions (fractions 9 and 10) were pooled and subjected to immunoprecipitation using anti-CD9 mAb. Immune complexes were electrophoresed on SDS-PAGE and probed with biotinylated anti-CD14 mAb, followed by streptavidin-conjugated peroxidase.

LPS challenge in vivo

In brief, 0.5 mg/kg LPS in 40 μl sterile PBS was intranasally administered to anesthetized mice. After 2 h-4 days, bronchoalveolar lavage was performed twice with 0.5 ml PBS. The recovered BALF was centrifuged and the supernatant was analyzed for cytokines and MMP activities. Cell pellets were resuspended in PBS, and total cell count and its subset analysis were performed using a hemocytometer and Diff-Quick stain (Sysmex), respectively. In another experiment, the cell pellets were resuspended in RPMI 1640 containing 2% FBS and cultured for 5 days. The cells were photographed, and morphologically activated macrophages were quantified by determining the percentage of spread cells with a process longer than 1-cell diameter (17).

Cytokine analysis

Concentrations of TNF-α in culture supernatants or BALF were measured by ELISA using Quantikine (R&D Systems). Multiple cytokine analysis of BALF was performed using mouse cytokine antibody array (MA6412; Panomics) according to the manufacturer's instructions. The signals were analyzed using the FluorChem.

Statistical analysis

In vitro assays were performed in quadruplicate cultures. Animal experiments were done using at least four mice for each group. All numerical results are expressed as mean ± SEM. Statistical differences were determined by Student's *t* test. p values <0.05 were considered statistically significant.

Results

Expression of macrophage CD9 and CD81 in the absence or presence of LPS

Signaling molecules in LPS-induced macrophage activation have been well characterized (1), but involvement of tetraspanin CD9 has not been studied. We first investigated macrophage expression of CD9 and its closely related tetraspanin, CD81, in the absence or presence of LPS. When a mouse macrophage line, RAW264.7, was treated with 0.1 μg/ml of LPS, cellular activation was noticeable with their morphological change (Fig. 1*A*). The cells were spread and extended long projections with time, whereas such prominent changes were not observed in the absence of LPS. Expressions of CD9 and CD81 were confirmed by immunoblotting, and it appeared that protein levels of CD9 and CD81 were transiently down-regulated in the presence of LPS, whereas their levels were relatively unchanged in the absence of LPS (Fig. 1*B*). We next isolated BMDMs from mice and examined the expression of CD9 and CD81. These tetraspanins were present in BMDMs, and LPS again down-regulated their levels moderately (Fig. 1*C*). We further isolated mouse alveolar macrophages by bronchoalveolar lavage and tested the effect of LPS in culture. Because the number of isolated cells was not enough for immunoblotting, the expression of CD9 and CD81 was examined by flow cytometry; the levels of CD9 and CD81 in mean fluorescence intensity were 136 and 45 before, and reduced to 112 and 36 at 48 h after LPS stimulation, respectively.

The loss of CD9 function exacerbates LPS-induced TNF-α and MMP production in vitro

LPS-induced macrophage activation leads to the production of proinflammatory mediators including cytokines and proteinases through the activation of NF-κB (1, 18). To elucidate a role of CD9 in LPS signaling, we negated CD9 function of RAW264.7 with mAb or siRNA transfection and examined the production of TNF-α and MMPs in vitro. As shown in Fig. 2*A*, treatment of RAW264.7 cells with a function-blocking anti-CD9 mAb, KMC8 (11), augmented LPS-induced secretion of TNF-α when compared with isotype-matched IgG. KMC8 also increased the basal level of TNF-α in the absence of LPS. siRNA transfection against CD9, which successfully knocked down CD9 protein in RAW264.7, likewise enhanced LPS-induced TNF-α secretion as well as its basal level (Fig. 2*B*). In addition, the CD9 knockdown increased LPS-induced MMP-9 activity in culture supernatants as shown in gelatin zymography and its densitometry analysis (Fig. 2*C*). MMP-2 activity was not detected in this cell line (19).

To extend the role of CD9 to primary macrophages, similar experiments were performed using BMDMs from WT and CD9 KO mice. These cells were stimulated with LPS and the production of TNF-α and MMPs was examined. Like the mAb- or siRNA-treated RAW264.7 cells, CD9 KO BMDMs secreted more TNF-α than WT counterparts when activated with LPS (Fig. 3*A*). By contrast with RAW264.7, these cells did not increase the basal level of TNF-α, possibly reflecting the difference between a cell line and primary cells. Meanwhile, the basal and LPS-induced expressions of MMP-2 and MMP-9 were both up-regulated in CD9 KO BMDMs when compared with WT cells in RT-PCR (Fig. 3*B*). Augmentation of the LPS-induced gelatinolytic activity of MMP-2

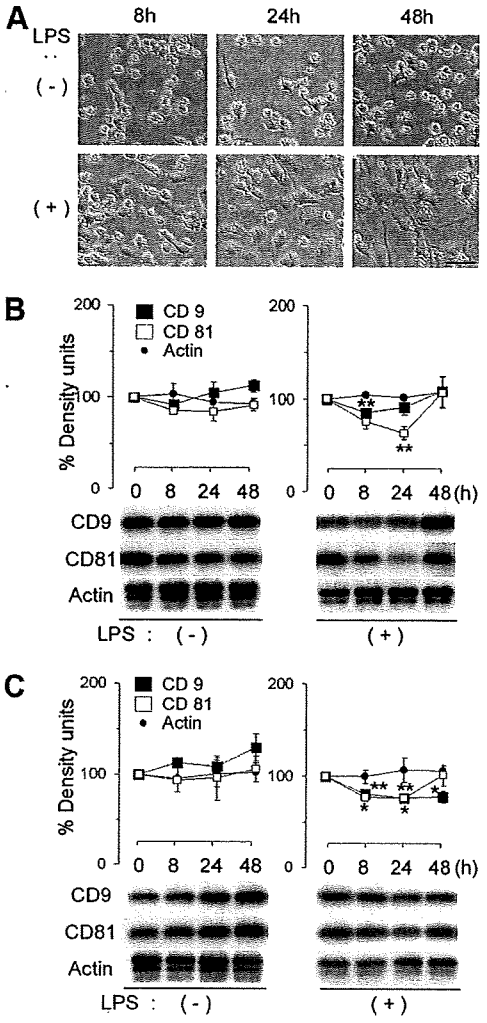

FIGURE 1. Expression of macrophage CD9 and CD81 in the absence or presence of LPS. *A*, RAW264.7 macrophages were serum-starved and cultured in the absence (−) or presence (+) of 0.1 μg/ml LPS. After the indicated hours, the cells were photographed. Bar, 50 μm. *B*, After the indicated hours, lysates of RAW264.7 cells were electrophoresed on SDS-PAGE and transferred to an Immobilon-P membrane. CD9 and CD81 were immunoblotted with anti-CD9 and anti-CD81 mAbs. Anti-actin blots show comparable amounts of protein loaded in each lane (*lower panels*). The intensity of blots was quantified by densitometry (*upper panels*). *C*, Mouse BMDMs were serum-starved and cultured in the absence or presence of 1 μg/ml LPS. After the indicated hours, the cells were lysed and protein levels of CD9 and CD81 were examined by immunoblotting (*lower panels*). The intensity of blots was quantified by densitometry (*upper panels*). Blots shown in the *lower panels* are from one representative of three independent experiments and each data point in the *upper panels* represents the mean ± SEM. ⋆, $p < 0.05$ vs 0 h; ⋆⋆, $p < 0.01$ vs 0 h. Asterisks for CD9 and CD81 are shown above and below symbols, respectively.

and MMP-9 was confirmed by zymography (Fig. 3*C*). We additionally tested alveolar macrophages isolated from BALF and again found that CD9 KO macrophages produce a higher level of TNF-α when activated with LPS in vitro (Fig. 3*D*).

CD14 expression and its association with TLR4 are enhanced in CD9 KO macrophages

CD14 is a major component of the LPS receptor complex, and it was previously reported that LPS binding to macrophages up-regulates the expression of CD14 (5). To explore mechanisms underlying the loss of CD9 function effect on LPS signaling, CD14

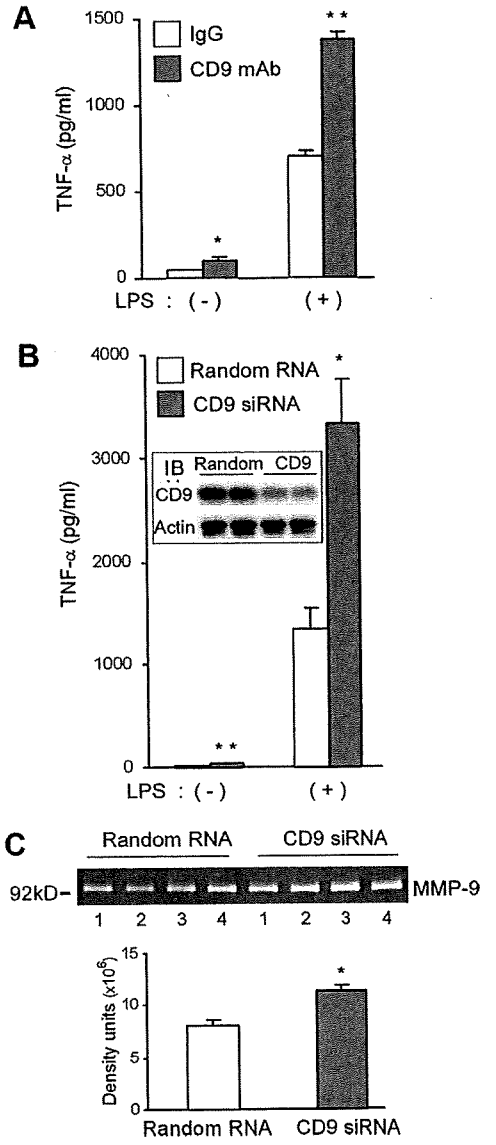

FIGURE 2. RAW264.7 cells treated with mAbs or siRNA transfection to CD9 produce more TNF-α and MMP-9 than control cells in vitro. *A*, RAW264.7 cells were treated with 10 μg/ml anti-CD9 mAb, KMC8, or isotype-matched IgG and cultured in the absence (−) or presence (+) of 0.1 μg/ml LPS. After 18 h, the concentration of TNF-α in culture supernatants was measured in ELISA. Data shown are from one representative of three similar experiments. *B*, RAW264.7 cells were transfected with siRNAs to CD9 or random RNAs, and knockdown of CD9 protein was confirmed twice in immunoblotting (*inset*). The transfected cells were cultured in the absence (−) or presence (+) of 0.1 μg/ml LPS. After 18 h, the concentration of TNF-α in culture supernatants was measured in ELISA. The assays were done in four independent transfections. *C*, RAW264.7 cells were transfected with siRNAs to CD9 or random RNAs, and the transfected cells were cultured in the presence of 0.1 μg/ml LPS. After 18 h, samples of culture supernatants were electrophoresed on a polyacrylamide gel containing 0.1% gelatin. The assays were done in four independent transfections. Gelatinolytic bands after these four transfections (1–4) were visualized by Coomassie brilliant blue R250 staining (*upper panel*), and the intensity of lytic bands of MMP-9 was quantified by densitometry (*lower panel*). Each bar represents the mean ± SEM. ⋆, $p < 0.05$ vs control; ⋆⋆, $p < 0.01$ vs control.

expression and its association with TLR4 were examined using BMDMs isolated from WT and CD9 KO mice. As shown in Fig. 4*A*, protein level of CD14 was slightly increased in naive CD9 KO

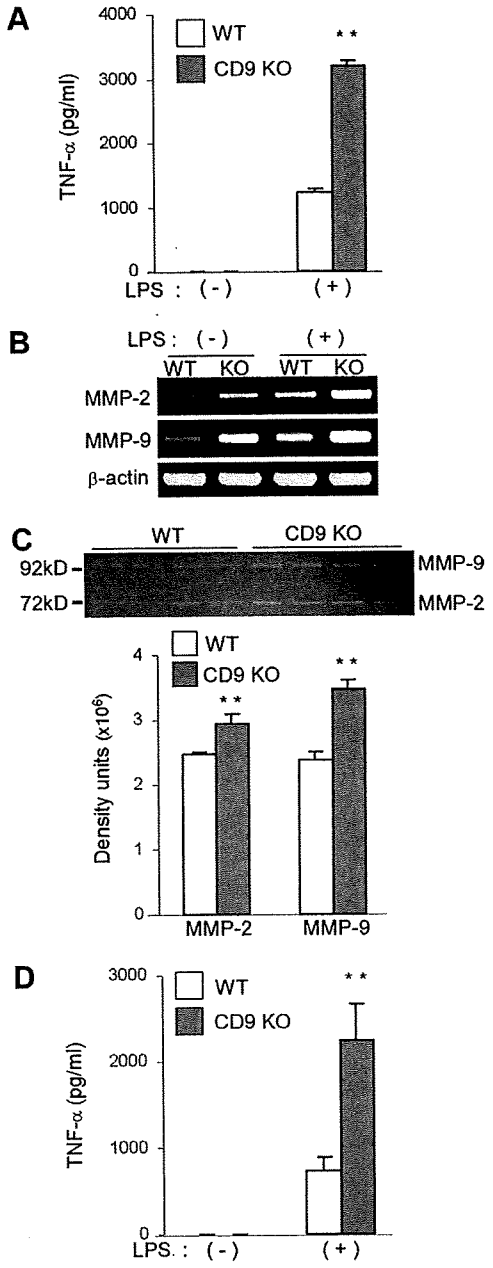

FIGURE 3. CD9 KO macrophages produce more TNF-α and MMPs than WT cells in vitro. *A*, BMDMs from WT and CD9 KO mice were cultured in the absence (−) or presence (+) of 1 μg/ml LPS. After 18 h, the concentration of TNF-α in culture supernatants was measured in ELISA. The assays were done using BMDMs collected from four mice for each group. *B*, BMDMs from WT and CD9 KO mice were cultured in the absence (−) or presence (+) of 1 μg/ml LPS. After 18 h, total RNA was extracted and analyzed for expressions of MMP-2 and MMP-9 by RT-PCR. β-actin amplification was used as the internal control. Data shown are from one representative of three similar experiments. *C*, BMDMs collected from WT and CD9 KO mice were cultured in the presence of 1 μg/ml LPS. After 18 h, aliquots of culture supernatants were electrophoresed in quadruplicate on a polyacrylamide gel containing 0.1% gelatin. Gelatinolytic bands were visualized by Coomassie brilliant blue R250 staining (*upper panel*), and the intensity of lytic bands of MMP-2 and MMP-9 was quantified by densitometry (*lower panel*). *D*, Alveolar macrophages from WT and CD9 KO mice were cultured in the absence (−) or presence (+) of 0.1 μg/ml LPS. After 24 h, the concentration of TNF-α in culture supernatants was measured in ELISA. The assays were done using alveolar macrophages from four mice for each group ($n = 4$). Each bar represents the mean ± SEM. ⋆⋆, $p < 0.01$ vs WT.

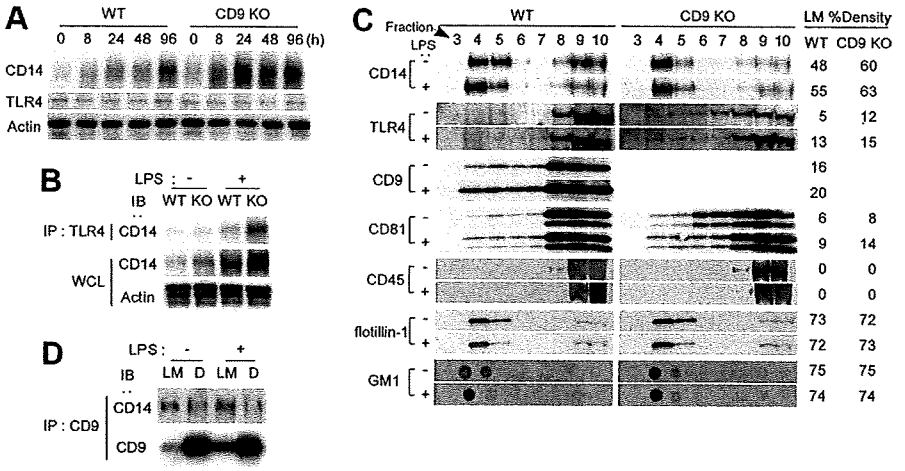

FIGURE 4. The expression of CD14, complex formation of CD14 and TLR4, and their localization into the lipid raft are enhanced in CD9 KO BMDMs. *A*, BMDMs from WT and CD9 KO mice were stimulated with 1 μg/ml LPS. After the indicated hours, cell lysates were electrophoresed on SDS-PAGE, transferred to a membrane, probed with anti-CD14 and anti-TLR4 Abs. Anti-actin blots show comparable amounts of protein loaded in each lane. *B*, WT and CD9 KO BMDMs were cultured in the absence (−) or presence (+) of LPS for 20 h. CD14 protein in whole cell lysates (WCL) and in immunoprecipitates with anti-TLR4 mAb (MTS510) was immunoblotted with biotinylated anti-CD14 Ab after SDS-PAGE. Anti-actin blots show comparable amounts of protein loaded in each lane. *C*, Cell lysates from WT and CD9 KO BMDMs cultured in the absence (−) or presence (+) of LPS for 2 h were centrifuged in sucrose density gradients. Fractions were collected from the top of the gradient and separated by SDS-PAGE. Protein distribution in the fractions was visualized by immunoblotting with anti-CD14, anti-TLR4, anti-CD9, anti-CD81, anti-CD45, and anti-flotillin-1 Abs. GM1 ganglioside was detected with HRP-conjugated cholera toxin by dot blot. The intensity of blots was quantified by densitometry. Percentage of density units of light membrane (LM) fractions (4 plus 5) were calculated and shown on the right of blots. *D*, Pooled LM fractions (4 and 5) and dense (D) fractions (9 and 10) from the sucrose gradients of WT cell lysate were subjected to imunoprecipiation with anti-CD9 mAb. After separation of the immunoprecipitates on SDS-PAGE, CD14 and CD9 were immunoblotted with biotinylated anti-CD14 Ab and anti-CD9 mAb, respectively. Data shown are from one representative of three similar experiments.

BMDMs, and LPS-induced CD14 up-regulation was enhanced compared with WT cells. Although the level of TLR4 remained unchanged (Fig. 4*A*), it coprecipitated a larger amount of CD14 protein in CD9 KO BMDMs after LPS stimulation (Fig. 4*B*, *upper panel*), most likely reflecting the increased expression of CD14 (Fig. 4*B*, *middle panel*) and its concentration to lipid rafts (see below).

Distribution of CD14 and TLR4 to the lipid raft is increased in CD9 KO macrophages

CD14 resides in lipid rafts in naive macrophages and, upon stimulation with LPS, more CD14 protein concentrates into the lipid rafts to form activation clusters with other signaling molecules including TLR4 (3, 4). Tetraspanins form their own multimolecular networks, TEM, which can interact with lipids, and thus tetraspanin complexes also appear within low-density light membrane fractions in sucrose gradients, especially when mild nonionic detergents are used (8). To study the localization into lipid and nonlipid microdomains before and after LPS stimulation, CD14, TLR4, CD9, and CD81 were immunoblotted using sucrose gradient fractions of BMDMs. In naive WT cells, CD14 resided both in light membrane fractions (fractions 4 and 5) and in dense fractions (fractions 9 and 10) (Fig. 4*C*, CD14, *left upper panel*). Proteins, although not all, in the former fractions were generally regarded as components of lipid rafts, as evidenced by the distribution of flotillin-1 and GM1 ganglioside into these fractions (Fig. 4*C*, flotillin-1 and GM1, *left panels*) (20, 21). Meanwhile, most TLR4 protein was distributed to dense fractions (Fig. 4*C*, TLR4, *left upper panel*). Upon LPS stimulation, portions of CD14 (Fig. 4*C*, CD14, *left lower panel*) and TLR4 (Fig. 4*C*, TLR4, *left lower panel*) were recruited from dense fractions to light membrane fractions as previously described (21, 4). Most CD9 and CD81 proteins were solubilized and localized at dense fractions in naive BMDMs, because a stringent nonionic detergent Triton X-100 was used (Fig. 4*C*, CD9 and CD81, *left upper panels*) (22). However, upon LPS stimulation, these tetraspanins were partly redistributed to light fractions like TLR4 (Fig. 4*C*, CD9 and CD81, *left lower panels*).

We next tested sucrose gradient fractions from CD9 KO BMDMs. Of note, when CD9 was completely absent, a larger portion of CD14 protein was already localized into light membrane fractions (Fig. 4*C*, CD14, *right upper panel*) compared with WT (Fig. 4*C*, CD14, *left upper panel*) even in naive BMDMs, and LPS stimulation slightly up-regulated CD14 of these fractions (Fig. 4*C*, CD14, *right lower panel*). The loss of CD9 also shifted the distribution of TLR4 and CD81 to light fractions (Fig. 4*C*, TLR4 and CD81, *right upper panels*) compared with WT BMDMs (Fig. 4*C*, TLR4 and CD81, *left upper panels*) before LPS stimulation. As a result, probably, more TLR4 and CD81 proteins localized into light membrane fractions (Fig. 4*C*, TLR4 and CD81, *right lower panels*) compared with WT (Fig. 4*C*, TLR4 and CD81, *left lower panels*) after LPS stimulation. Densitometry supplements the immunoblots quantitatively indicating the shift of these proteins to light membrane fractions (Fig. 4*C*, LM % density units). By contrast, the distribution of GM1 ganglioside and a raft-marker protein, flotillin-1, was not affected by the absence of CD9 (Fig. 4*C*, flotillin-1 and GM1, *right panels*) when compared with WT (Fig. 4*C*, GM1 and flotillin-1, *left panels*). Also, the loss of CD9 did not affect the distribution of a nonraft protein, CD45 (23) (Fig. 4*C*, CD45, *right panels*), compared with WT (Fig. 4*C*, CD45, *left panels*).

The codistribution of CD9 and CD14 into light membrane fractions, especially after LPS stimulation, raises a possible interaction between these two molecules in WT macrophages. Thus, we performed coprecipitation experiments using pooled light membrane fractions and dense fractions. Of note, more CD14 protein coprecipitated with CD9 in the light fractions than in the dense fractions before and after LPS stimulation (Fig. 4*D*), suggesting physical

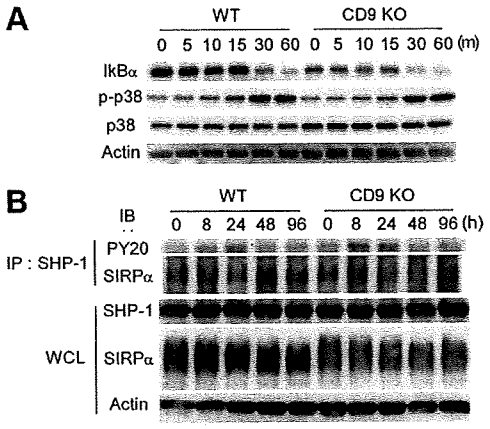

FIGURE 5. Accelerated IκB degradation and analysis of other signaling molecules in LPS-activated CD9 KO BMDMs. *A*, BMDMs from WT and CD9 KO mice were stimulated with 1 μg/ml LPS. After the indicated minutes, cell lysates were separated by SDS-PAGE, transferred to a membrane, and immunoblotted with anti-IκBα, anti-phosphorylated p38 (p-p38), and anti-p38 polyclonal Abs. Anti-actin blots show comparable amounts of protein loaded in each lane. *B*, SHP-1 was immunoprecipitated using anti-SHP-1 polyclonal Ab from cell lysates of WT and CD9 KO BMDMs stimulated with LPS for the indicated hours. After electrophoresis on SDS-PAGE and transfer to a membrane, tyrosine-phosphorylated SHP-1 was probed with anti-phosphotyrosine mAb (PY20), and the associated SIRPα was blotted with anti-SIRPα polyclonal Ab. SHP-1 and SIPRα in whole cell lysates (WCL) were immunoblotted in parallel. Anti-actin blots show comparable amounts of protein loaded in each lane. Data shown are from one representative of three similar experiments.

proximity between CD9 and CD14 in Triton X-100 lysate. These results suggest that CD9 may interfere with CD14 and the CD9 deficiency facilitates CD14-mediated receptor assembly at the lipid-enriched microdomain.

IκB degradation is accelerated in CD9 KO macrophages

Signals from LPS-induced CD14/TLR4 receptor complex lead to the degradation of IκB and result in release and translocation of NF-κB to the nucleus, where it activates proinflammatory genes including TNF-α and IL-6 (1). To examine whether CD9 prevents this LPS-induced NF-κB activation, protein level of IκBα was investigated by immunoblotting. As shown in Fig. 5*A*, IκBα was decreased before and degraded earlier after LPS stimulation in CD9 KO BMDMs than in WT cells, suggesting that CD9 deficiency accelerates NF-κB-mediated inflammatory response. Because LPS binding to macrophages also causes translocation of MAPK including ERK2 and p38 to the lipid raft and induces their activation (1, 21), we examined LPS-induced p38 phosphorylation in parallel. However, no difference was observed between WT and CD9 KO BMDMs (Fig. 5*A*).

SIRPα, a member of SIRP family, is abundantly expressed in macrophages and regulates LPS-induced macrophage activation and lung inflammation through association with a phosphotyrosine phosphatase, SHP-1 (24, 25). We additionally examined the activation of these signaling molecules in WT and CD9 KO BMDMs. No obvious difference was detected in phosphorylation of SHP-1 and its association with SIRPα. However, the total level of SIRPα protein appeared to be slightly lower in CD9 KO BMDMs throughout the LPS stimulation by unknown mechanisms (Fig. 5*B*).

Disruption of lipid-rich microdomains negates the enhanced TNF-α production in CD9 KO macrophages

β-cyclodextrins are a class of heptasaccharides commonly used to selectively remove cholesterol from cellular membranes, and partial depletion of cholesterol by β-cyclodextrins results in a loss of protein localization into lipid-rich microdomains (22). To investigate whether the disruption of lipid membrane microdomains leads to inhibition on macrophage response to LPS, BMDMs were cultured in the presence of 10 mM 2OHpβCD, and their TNF-α production into culture supernatants was quantified as previously described (26). We confirmed that this concentration of 2OHpβCD did not affect cell viability using MTT and lactate dehydrogenase assays (data not shown). As shown in Fig. 6*A*, 2OHpβCD strongly inhibited the LPS-induced TNF-α secretion both in WT and CD9 KO BMDMs and negated the enhanced secretion of CD9 KO BMDMs. The TNF-α secretion was also completely suppressed with a specific inhibitor of IκB kinase, BMS345541, indicating the total dependency on NF-κB activation. In an additional experiment, BMDMs were reloaded with cholesterol after the treatment of 2OHpβCD, and the enhanced TNF-α production reappeared in CD9 KO cells (Fig. 6*B*). These results suggest that lipid-enriched

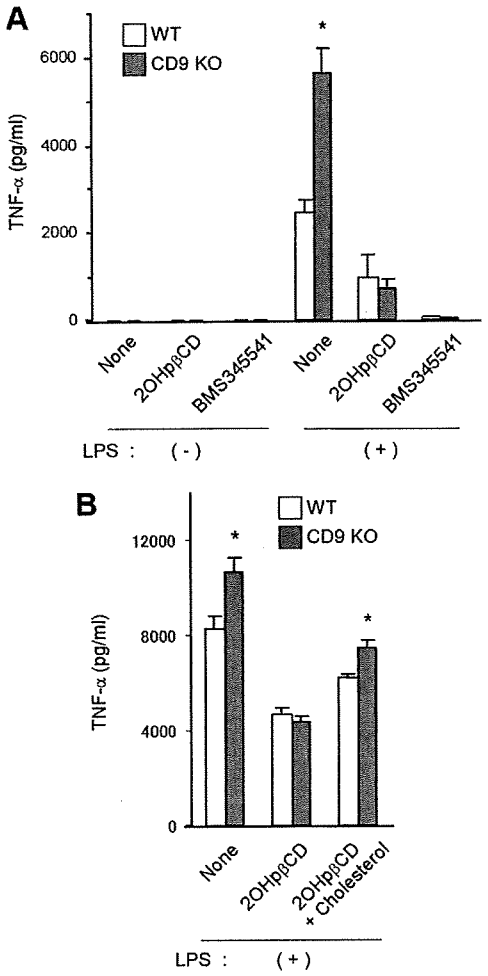

FIGURE 6. Cholesterol depletion inhibits LPS-induced, NF-κB-dependent production of TNF-α. *A*, BMDMs from WT and CD9 KO mice were untreated (None) or pretreated with 10 mM 2OHpβCD or 1 μM BMS345541 and cultured in the absence (−) or presence (+) of 1 μg/ml LPS. After 24 h, the concentration of TNF-α in culture supernatants was measured in ELISA. *B*, BMDMs were untreated (None), pretreated with 10 mM 2OHpβCD (2OHpβCD), or reloaded with cholesterol after the 2OHpβCD treatment (2OHpβCD + cholesterol), and then stimulated with LPS. After 24 h, the concentration of TNF-α in culture supernatants was measured in ELISA. The assays were done using BMDMs collected from four mice for each group. Each bar represents the mean ± SEM. ★, $p < 0.05$ vs WT.

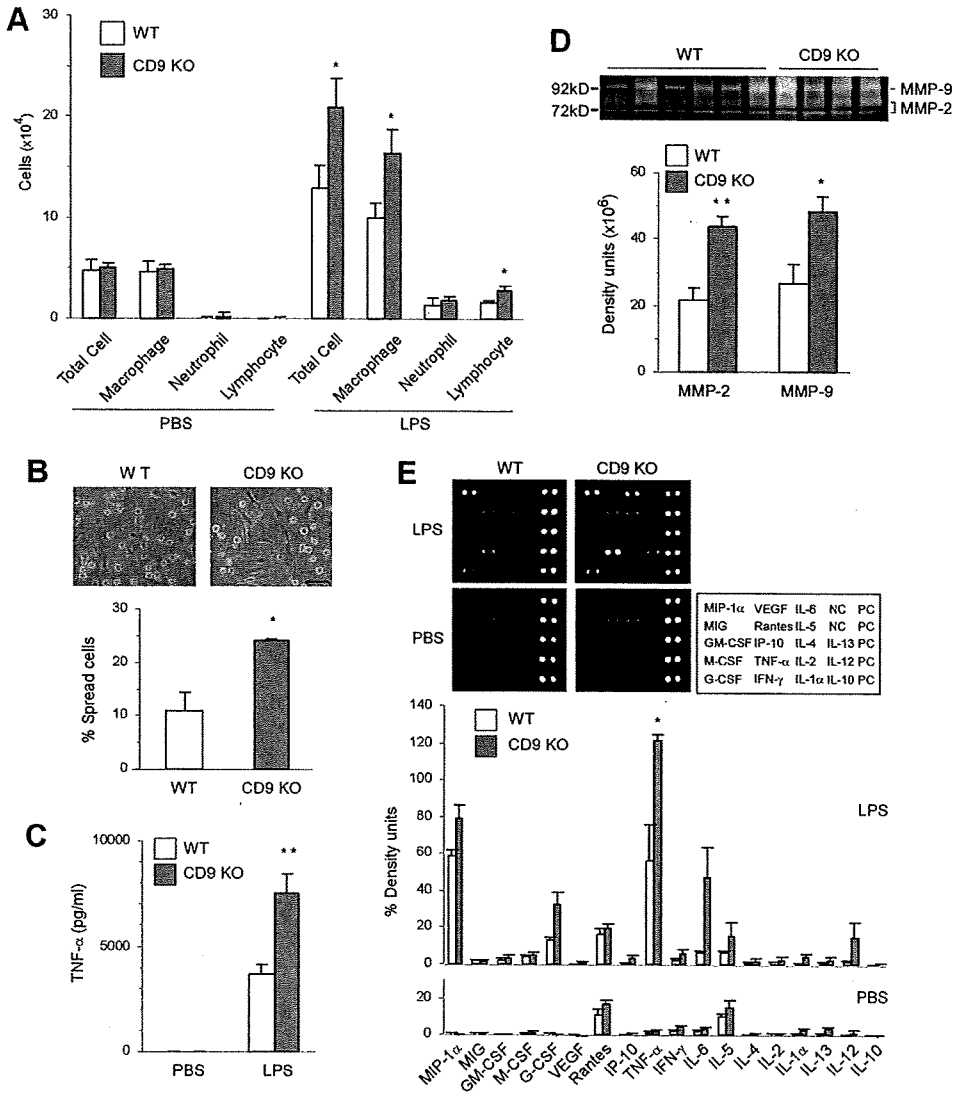

FIGURE 7. CD9 KO mice show exacerbated lung inflammation after intranasal administration of LPS in vivo. *A*, CD9 KO mice and WT littermates were challenged with intranasal administration of PBS or 0.5 mg/kg LPS. After 4 days, the lungs were lavaged, and total cell count and its subset analysis in BALF were performed using a hemocytometer and Diff-Quick stain, respectively. The assays were done using BALF from nine mice for each group ($n = 9$). *B*, After 2 days of the LPS administration to WT and CD9 KO mice, macrophages in the BALF were further cultured for 5 days and photographed (*upper panels*). The percentage of spread macrophages with a process longer than 1-cell diameter was determined (*lower panel*). The assays were done using BALF from four mice for each group ($n = 4$). The photos are from one representative of each group. Bar, 50 μm. *C*, After 2 h of the PBS or LPS administration to WT and CD9 KO mice, the concentration of TNF-α in the BALF was measured in ELISA. The assays were done using BALF from six mice for each group ($n = 6$). *D*, After 2 days of the LPS administration to WT and CD9 KO mice, samples of BALF from individuals of WT and CD9 KO mice were electrophoresed on a polyacrylamide gel containing 0.1% gelatin. Gelatinolytic bands were visualized by Coomassie brilliant blue R250 staining (*upper panel*), and the intensity of lytic bands of MMP-2 and MMP-9 was quantified by densitometry (*lower panel*). *E*, After 2 h of the PBS or LPS administration to WT and CD9 KO mice, multiple cytokines in the BALF were analyzed using mouse cytokine Ag array (*upper panels*) and its densitometry (*lower panels*). The position of cytokines in each array was shown in the *upper right panel*. PC, positive control; NC, negative control. Percentage of density units in *lower panels* were determined when the density of PC and NC was set at 100 and 0 units, respectively. The assays were done using BALF from four mice for each group ($n = 4$) and in duplicate for each mouse. The *upper left panels* are from one representative of each group. Each bar represents the mean ± SEM. ⋆, $p < 0.05$ vs WT; ⋆⋆, $p < 0.01$ vs WT.

microdomains provide an essential platform for CD9 to modulate LPS-induced macrophage activation.

The loss of CD9 exacerbates LPS-induced lung inflammation and production of cytokines and MMPs in vivo

Last, we investigated whether CD9 prevents LPS-induced lung inflammation in vivo. LPS was intranasally administered to CD9 KO mice and WT littermates and, 4 days later, histological lung sections from these mice were analyzed. Although neutrophil influx was observed earlier, cells dominantly infiltrating in the lung at this phase were macrophages (27), and we could not find marked histological difference between WT and CD9 KO mice (data not shown). However, when cells isolated from BALF and their subsets were analyzed, there was a clear difference. Whereas no difference was detected in control PBS administration, CD9 KO mice showed enhanced infiltration of inflammatory cells, most of which were macrophages, after the LPS challenge (Fig. 7*A*). Moreover, when alveolar macrophages isolated from the BALF were plated and cultured, the number of morphologically activated cells, which were spread and extended long projections, was larger in CD9 KO

mice compared with WT mice (Fig. 7*B*). The concentration of TNF-α in BALF revealed 2-fold increase in CD9 KO mice at 2 h after the LPS stimulation (Fig. 7*C*). Gelatin zymography using the BALF showed enhanced MMP-2 and MMP-9 activities in CD9 KO mice (Fig. 7*D*). We further evaluated expression profiles of multiple cytokines in the BALF using Cytokine Antibody Array. Consistent with the results of ELISA (Fig. 7*C*), a 2-fold increase in TNF-α was observed after the LPS administration in CD9 KO mice (Fig. 7*E*). Other macrophage cytokines including MIP-1α, G-CSF, IL-6, and IL-12 also appeared to be increased, although not statistically significant ($p < 0.1$ vs WT in all these cytokines). These results indicate that LPS-induced lung inflammation was exacerbated in CD9 KO mice compared with WT mice.

Discussion

In the present study, we firstly examined the expressions of tetraspanins CD9 and CD81 in cultured macrophages. The expression pattern was relatively different between the absence and presence of LPS (Fig. 1); when treated with LPS, these tetraspanins were transiently and moderately down-regulated in a cell line, RAW264.7, and primary macrophages. This down-regulation was concurrent with morphological activation. Based on the dogma that the tetraspanins form complexes with integrins and regulate cellular events involving cytoskeletal reorganization such as cell fusion and motility (7), we speculated that CD9 and CD81 may play a role in LPS-induced macrophage activation. To further clarify the role of the tetraspanins, we negated function of CD9 by mAb and siRNA treatment of RAW264.7 (Fig. 2) or by using KO macrophages (Fig. 3) and assessed the LPS response in vitro. In either case, LPS-induced production of proinflammatory mediators, TNF-α and MMPs, was augmented. Furthermore, in vivo deletion of CD9 in mice exacerbated LPS-induced lung inflammation, which was characterized by the infiltration of activated macrophages and overproduction of TNF-α and MMPs (Fig. 7). These results indicate that macrophage CD9 plays a negative role in the LPS response.

It has been recognized that membrane microdomains are important in LPS signaling (3). LPS stimulation of macrophages induces translocation of CD14 to the lipid raft and facilitates the formation of multimeric receptor complexes containing CD14, TLR4, and CD11b/CD18 (21). Meanwhile, tetraspanins including CD9 and CD81 also facilitate the formation of their own multimolecular protein network, designated TEM, at lipid-enriched microdomains. Although protein components at the raft and TEM can be localized at low-density light membrane fractions in sucrose gradients, it is thought that these two microdomains are distinct in view of several aspects. For example, lipid rafts are disrupted at 37°C, whereas TEMs are maintained. Lipid rafts are typically insoluble in nonionic detergents, whereas TEMs are mostly soluble in nonionic detergents (8). However, recent data suggest that there may be an overlapping or an interaction between the raft and TEM proteins under certain conditions (9, 28, 10). Such interactions may result in the close proximity of these distinct sets of membranous molecules and facilitate signal transduction (10). Indeed, regulations of the lipid raft and TEM were both shown to be dynamic upon cellular activation in previous studies (3, 11). In the present study, most CD9 and CD81 proteins were soluble in Triton X-100 and distributed in dense sucrose gradient fractions, and a small portion of these protein resided in light fractions in naive BMDMs. Importantly, upon LPS stimulation, more CD9 and CD81 protein concentrated into the light fractions, where raft proteins also assemble. The coprecipitation experiments revealed a physical proximity between CD9 and CD14 in the light fractions but not in the dense fractions (Fig. 4). Thus, there might be a specialized lipid microdomain, where the raft and TEM interact, especially upon LPS stimulation.

The experiments using CD9 KO macrophages indicated that the loss of CD9 enhances LPS-induced signaling in at least two different ways (Fig. 4). First, the protein level of CD14 was increased in naive CD9 KO BMDMs, and its up-regulation with LPS was enhanced when compared with WT cells. LPS-induced increase of CD14 expression occurs at the mRNA level in RAW264.7 macrophages (5), but whether the further elevation of CD14 in the absence of CD9 occurs at the mRNA or protein level remains to be investigated. Second, larger portions of CD14 and TLR4 proteins were concentrated into light membrane fractions relative to dense fractions in CD9 KO BMDMs than in WT cells. CD9 is an abundantly expressed tetraspanin in macrophages (29) and, in WT BMDMs, the population of CD9 molecules recruited into the lipid-rich microdomains would not be small. So, the absence of CD9 might remove its direct interference with CD14 signaling complexes at the microdomains. These alterations most likely increase functional CD14/TLR4 receptor clusters, the composition and stoichiometry of which are important determinants for immune response (20). Thus, we speculate that CD9 KO BMDMs are in "primed" conditions and, upon LPS binding, they are easily and rapidly activated. The platform where CD9 regulates the LPS response is a cholesterol-enriched microdomain, and this is essential for the CD9 function because the level of TNF-α production of CD9 KO BMDMs was reduced to the same level as WT cells after cholesterol depletion with 2OHpβCD (Fig. 6). Collectively, it seems that macrophage CD9 negatively regulates the LPS response by preventing CD14-mediated signaling at lipid-enriched microdomains.

Among other signaling molecules tested, the expression of SIRPα appeared slightly lower in CD9 KO BMDMs (Fig. 5). A recent report showed that the SIRPα level of macrophages is important to regulate LPS signaling negatively at an early stage of TLR4 activation (30). Although detailed mechanisms remain to be studied, there is a possibility that the decreased SIRPα may also participate in CD9-mediated negative regulation of LPS response.

CD81 is another macrophage tetraspanin closely related to CD9 (7). This tetraspanin showed the redistribution similar to CD9 in sucrose gradients; a portion of CD81 protein was concentrated to light membrane fractions upon LPS stimulation (Fig. 4). Interestingly, in CD9 KO BMDMs, CD81 distribution was shifted to light fractions compared with WT cells (Fig. 4). Possibly, this might mean CD81 compensates for the loss of CD9 function at lipid microdomains as proposed previously (7). Using a fluorescence resonance energy transfer technique, participation of CD81 into the CD14/TLR4 receptor clustering at the lipid membrane microdomain has been reported in previous studies (15, 3, 20). These studies displayed that stimulation of human monocytes with LPS induced coassembly of CD14, TLR4, CD11b/CD18, CD81, and other molecules in vitro, although the meaning of the CD81 participation remained unknown. They further provided data suggesting a coassembly of CD81 and CD14 in monocytes from patients with sepsis (i.e., in vivo LPS stimulation) (15). CD9 was also examined in their recent study (28) but, unlike the present study, CD9 appeared not to be associated with the lipid microdomain in a rapid detergent-based flow cytometric assay. This discrepancy may be due to methodological differences or might be because they used human monocytes from healthy donors (i.e., without in vivo LPS stimulation) in this CD9 experiment (28). Studies using CD81 KO macrophages and, hopefully, CD9/CD81 double-KO macrophages, will be needed to delineate coordination of tetraspanins CD9 and CD81 in the LPS-induced CD14 signaling.

In conclusion, we have shown that LPS-induced lung inflammation is exacerbated in the absence of CD9 function. As part of its mechanisms, we propose that CD9 negatively regulates LPS-induced macrophage activation by preventing CD14-dependent receptor assembly at lipid-enriched membrane microdomains. LPS is one of molecules contained by cigarette smoke that leads to pulmonary emphysema, and also causes fatal sepsis syndrome including acute lung injury in humans. Thus, the deficiency of CD9 function may be an important predisposing factor to such inflammatory lung diseases.

Acknowledgments

We thank Dr. E. Mekada for generously providing CD9 KO mice and helpful comments on this paper, and Y. Habe for secretarial assistance.

Disclosures

The authors have no financial conflict of interest.

References

1. Fujihara, M., M. Muroi, K. Tanamoto, T. Suzuki, H. Azuma, and H. Ikeda. 2003. Molecular mechanisms of macrophage activation and deactivation by lipopolysaccharide: roles of the receptor complex. *Pharmacol. Ther.* 100: 171–194.
2. Triantafilou, M., and K. Triantafilou. 2002. Lipopolysaccharide recognition: CD14, TLRs and the LPS-activation cluster. *Trends Immunol.* 23: 301–304.
3. Schmitz, G., and E. Orso. 2002. CD14 signalling in lipid rafts: new ligands and co-receptors. *Curr. Opin. Lipidol.* 13: 513–521.
4. Szabo, G., A. Dolganiuc, Q. Dai, and S. B. Pruett. 2007. TLR4, ethanol, and lipid rafts: a new mechanism of ethanol action with implications for other receptor-mediated effects. *J. Immunol.* 178: 1243–1249.
5. Frey, T., and A. De Maio. 2007. Increased expression of CD14 in macrophages after inhibition of the cholesterol biosynthetic pathway by lovastatin. *Mol. Med.* 13: 592–604.
6. Levy, S., and T. Shoham. 2005. Protein-protein interactions in the tetraspanin web. *Physiology* 20: 218–224.
7. Hemler, M. E. 2003. Tetraspanin proteins mediate cellular penetration, invasion, and fusion events and define a novel type of membrane microdomain. *Annu. Rev. Cell Dev. Biol.* 19: 397–422.
8. Hemler, M. E. 2005. Tetraspanin functions and associated microdomains. *Nat. Rev. Mol. Cell Biol.* 6: 801–811.
9. Ishii, M., K. Iwai, M. Koike, S. Ohshima, E. Kudo-Tanaka, T. Ishii, T. Mima, Y. Katada, K. Miyatake, Y. Uchiyama, and Y. Saeki. 2006. RANKL-induced expression of tetraspanin CD9 in lipid raft membrane microdomain is essential for cell fusion during osteoclastogenesis. *J. Bone Miner. Res.* 21: 965–976.
10. Israels, S. J., and E. M. McMillan-Ward. 2007. Platelet tetraspanin complexes and their association with lipid rafts. *Thromb. Haemost.* 98: 1081–1087.
11. Takeda, Y., I. Tachibana, K. Miyado, M. Kobayashi, T. Miyazaki, T. Funakoshi, H. Kimura, H. Yamane, Y. Saito, H. Goto, et al. 2003. Tetraspanins CD9 and CD81 function to prevent the fusion of mononuclear phagocytes. *J. Cell Biol.* 161: 945–956.
12. Takeda, Y., P. He, I. Tachibana, B. Zhou, K. Miyado, H. Kaneko, M. Suzuki, S. Minami, T. Iwasaki, S. Goya, et al. 2008. Double deficiency of tetraspanins CD9 and CD81 alters cell motility and protease production of macrophages and causes chronic obstructive pulmonary disease-like phenotype in mice. *J. Biol. Chem.* 283: 26089–26097.
13. Miyado, K., G. Yamada, S. Yamada, H. Hasuwa, Y. Nakamura, F. Ryu, K. Suzuki, K. Kosai, K. Inoue, A. Ogura, et al. 2000. Requirement of CD9 on the egg plasma membrane for fertilizaion. *Science* 287: 321–324.
14. Kobayashi, K., L. D. Hernandez, J. E. Galan, C. A. Janeway, Jr., R. Medzhitov, and R. A. Flavell. 2002. IRAK-M is a negative regulator of Toll-like receptor signaling. *Cell* 110: 191–202.
15. Pfeiffer, A., A. Bottcher, E. Orso, M. Kapinsky, P. Nagy, A. Bodnar, I. Spreitzer, G. Liebisch, W. Drobnik, K. Gempel, et al. 2001. Lipopolysaccharide and ceramide docking to CD14 provokes ligand-specific receptor clustering in rafts. *Eur. J. Immunol.* 31: 3153–3164.
16. Shibata, Y., Z. Zsengeller, K. Otake, N. Palaniyar, and B. C. Trapnell. 2001. Alveolar macrophage deficiency in osteopetrotic mice deficient in macrophage colony-stimulating factor is spontaneously corrected with age and associated with matrix metalloproteinase expression and emphysema. *Blood* 98: 2845–2852.
17. Tachibana, I., M. Mori, Y. Tanio, S. Hosoe, T. Sakuma, T. Osaki, K. Ueno, T. Kumagai, T. Kijima, and T. Kishimoto. 1996. A 100-kDa protein tyrosine phosphorylation is concurrent with β1 integrin-mediated morphological differentiation in neuroblastoma and small cell lung cancer cells. *Exp. Cell Res.* 227: 230–239.
18. Rhee, J. W., K. W. Lee, D. Kim, Y. Lee, O. H. Jeon, H. J. Kwon, and D. S. Kim. 2007. NF-κB-dependent regulation of matrix metalloproteinase-9 gene expression by lipopolysaccharide in a macrophage cell line RAW 264.7. *J. Biochem. Mol. Biol.* 40: 88–94.
19. Ogawa, K., F. Chen, C. Kuang, and Y. Chen. 2004. Suppression of matrix metalloproteinase-9 transcription by transforming growth factor-β is mediated by a nuclear factor-κB site. *Biochem. J.* 381: 413–422.
20. Triantafilou, M., K. Brandenburg, S. Kusumoto, K. Fukase, A. Mackie, U. Seydel, and K. Triantafilou. 2004. Combinational clustering of receptors following stimulation by bacterial products determines lipopolysaccharide responses. *Biochem. J.* 381: 527–536.
21. Olsson, S., and R. Sundler. 2006. The role of lipid rafts in LPS-induced signaling in a macrophage cell line. *Mol. Immunol.* 43: 607–612.
22. Claas, C., C. S. Stipp, and M. E. Hemler. 2001. Evaluation of prototype transmembrane 4 superfamily protein complexes and their relation to lipid rafts. *J. Biol. Chem.* 276: 7974–7984.
23. Rodgers, W., and J. K. Rose. 1996. Exclusion of CD45 inhibits activity of p56lck associated with glycolipid-enriched membrane domains. *J. Cell Biol.* 135: 1515–1523.
24. Smith, R. E., V. Patel, S. D. Seatter, M. R. Deehan, M. H. Brown, G. P. Brooke, H. S. Goodridge, C. J. Howard, K. P. Rigley, W. Harnett, and M. M. Harnett. 2003. A novel MyD-1 (SIRP-1α) signaling pathway that inhibits LPS-induced TNFα production by monocytes. *Blood* 102: 2532–2540.
25. Hardin, A. O., E. A. Meals, T. Yi, K. M. Knapp, and B. K. English. 2006. SHP-1 inhibits LPS-mediated TNF and iNOS production in murine macrophages. *Biochem. Biophys. Res. Commun.* 342: 547–555.
26. Koseki, M., K. Hirano, D. Masuda, C. Ikegami, M. Tanaka, A. Ota, J. C. Sandoval, Y. Nakagawa-Toyama, S. B. Sato, T. Kobayashi, et al. 2007. Increased lipid rafts and accelerated lipopolysaccharide-induced tumor necrosis factor-α secretion in Abca1-deficient macrophages. *J. Lipid Res.* 48: 299–306.
27. Liang, J., D. Jiang, J. Griffith, S. Yu, J. Fan, X. Zhao, R. Bucala, and P. W. Noble. 2007. CD44 is a negative regulator of acute pulmonary inflammation and lipopolysaccharide-TLR signaling in mouse macrophages. *J. Immunol.* 178: 2469–2475.
28. Wolf, Z., E. Orso, T. Werner, H. H. Klunemann, and G. Schmitz. 2007. Monocyte cholesterol homeostasis correlates with the presence of detergent resistant membrane microdomains. *Cytometry A* 71: 486–494.
29. Wang, X. Q., G. F. Evans, M. L. Alfaro, and S. H. Zuckerman. 2002. Down-regulation of macrophage CD9 expression by interferon-γ. *Biochem. Biophys. Res. Commun.* 290: 891–897.
30. Kong, X. N., H. X. Yan, L. Chen, L. W. Dong, W. Yang, Q. Liu, L. X. Yu, D. D. Huang, S. Q. Liu, H. Liu, et al. 2007. LPS-induced down-regulation of signal regulatory protein α contributes to innate immune activation in macrophages. *J. Exp. Med.* 204: 2719–2731.

Cancer Science
The official journal of the Japanese Cancer Association JCA

Decreased infiltration of macrophage scavenger receptor-positive cells in initial negative biopsy specimens is correlated with positive repeat biopsies of the prostate

Norio Nonomura,[1,3] Hitoshi Takayama,[1] Atsunari Kawashima,[1] Masatoshi Mukai,[1] Akira Nagahara,[1] Yasutomo Nakai,[1] Masashi Nakayama,[1] Akira Tsujimura,[1] Kazuo Nishimura,[1] Katsuyuki Aozasa[2] and Akihiko Okuyama[1]

Departments of [1]Urology, [2]Pathology, Osaka University Graduate School of Medicine, Osaka, Japan

(Received January 15, 2010/Revised February 26, 2010/Accepted March 3, 2010/Accepted manuscript online March 15, 2010)

Macrophage scavenger receptor (MSR)-positive inflammatory cells and tumor-associated macrophages (TAMs) have been reported to regulate the growth of various cancers. In this study, the infiltration of MSR-positive cells and TAMs was analyzed to predict the outcome of repeat biopsy in men diagnosed as having no malignancy at the first prostate biopsy. Repeat biopsy of the prostate was carried out in 92 patients who were diagnosed as having no malignancy at the first biopsy. Of these, 30 patients (32.6%) were positive for prostate cancer at the repeat biopsy. Tumor-associated macrophages and MSR-positive cells were immunohistochemically stained with mAbs CD68 and CD204, respectively. Six ocular measuring fields were chosen randomly under a microscope at ×400 power in the initial negative biopsy specimens, and the mean TAM and MSR counts for each case were determined. No difference in TAM count was found between the cases with or without prostate cancer. By contrast, the MSR count in patients with cancer was significantly lower than that in patients without cancer at the repeat biopsy ($P < 0.001$). Logistic regression analysis indicated that the MSR count at first biopsy is a significantly better predictive factor for positive repeat biopsy than PSA velocity, interval between first and repeat biopsies, or TAM count. Decreased infiltration of MSR-positive cells in negative first biopsy specimens was correlated with positive findings in the repeat biopsy. The MSR count might be a good indicator for avoiding unnecessary repeat biopsies. (*Cancer Sci* 2010)

Prostate cancer (PCa) is one of the most common cancers in males in developed countries.[1] Prostate-specific antigen (PSA) is currently the most useful serum tumor marker for detecting Pca.[2] However, because of the low specificity of PSA, many patients undergo unnecessary needle biopsies of the prostate.[3] Most patients who undergo prostate biopsies and have negative pathological findings are followed up with periodic PSA measurements. A repeat biopsy might be indicated by the presence of high-grade prostatic intraepithelial neoplasia (HGPIN) on the initial biopsy, a low percentage of free PSA, an increasing PSA velocity, elevated PSA density, or changes on digital rectal examination.[4–8] Several additional biomarkers and molecular markers prompt us to carry out a repeat biopsy, including prostate cancer gene 3 mRNA in the urine,[9,10] hypermethylation of the glutathione S-transferase pi 1 gene promoter in post-biopsy urine specimens,[11] and telomerase activity in prostate massage samples.[12]

Recurrent or chronic inflammation has been implicated in the development of many human cancers, including gastric, liver, colon, and urinary bladder cancers.[13] It has been reported that some inflammatory cells contribute positively to carcinogenesis or cancer progression in the prostate.[14–17] Of the many kinds of inflammatory cell, decreased infiltration of macrophage scavenger receptor 1 (MSR1)-positive cells has been reported to play important roles in the progression of PCa.[18] Germ-line mutations in the *MSR1* gene leading to defective expression are involved in prostate carcinogenesis.[19–21] Therefore, we examined the association between tumor-associated macrophage (TAM) infiltration or the expression of MSR1 and the rate of detection of PCa at a repeat biopsy of the prostate in patients in whom the first biopsy was negative.

Materials and Methods

Patients. Between 1997 and 2000, 373 patients underwent first prostate biopsy because of elevated serum PSA, positive digital rectal examination (DRE), or positive findings in transrectal ultrasonography. Of these, 222 patients (59.5%) with negative biopsy were followed up periodically (usually at 6-month intervals) with a serum PSA check or DRE. From this group, 92 patients (42.8%) ranging in age from 51 to 82 years (median, 69 years) underwent repeat biopsies of the prostate because of the increasing serum PSA level, appearance of abnormal nodules in the prostate by DRE, or their anxiety. Of these 92 patients, 30 (32.6%) were positive for cancer at the repeat biopsy. Written informed consent was obtained from all patients.

Immunohistochemistry. Biopsy specimens were fixed in 10% neutral buffered formalin and routinely processed for paraffin embedding. Serial 5-μm-thick sections were cut, and one section was stained with H&E and reviewed by a pathologist (K.A., one of the authors) to obtain the pathological diagnosis. Tumor-associated macrophages and MSR-positive inflammatory cells were labeled immunohistochemically using mAbs CD68 (1:100 dilution; Dako, Glostrup, Denmark) and CD204 (1:100 dilution; Trans Genic, Kobe, Japan), respectively, and were visualized using an LSAB kit (Dako). For systematic counting, six ocular measuring fields, each with a real area of 0.06175 mm^2, were chosen randomly under a microscope at ×400 in the first negative biopsy specimens. For each case, the mean numbers of the TAMs and MSR-positive cells were determined as the TAM and MSR count of each case.

Statistical analysis. Statistical analysis was carried out using StatView (SAS Institute, Cary, NC, USA). Differences in the PSA value, TAM count, and MSR count between the cancer and normal groups were evaluated using the Mann–Whitney *U*-test.

[3]To whom correspondence should be addressed.
E-mail: nono@uro.med.osaka-u.ac.jp

doi: 10.1111/j.1349-7006.2010.01563.x

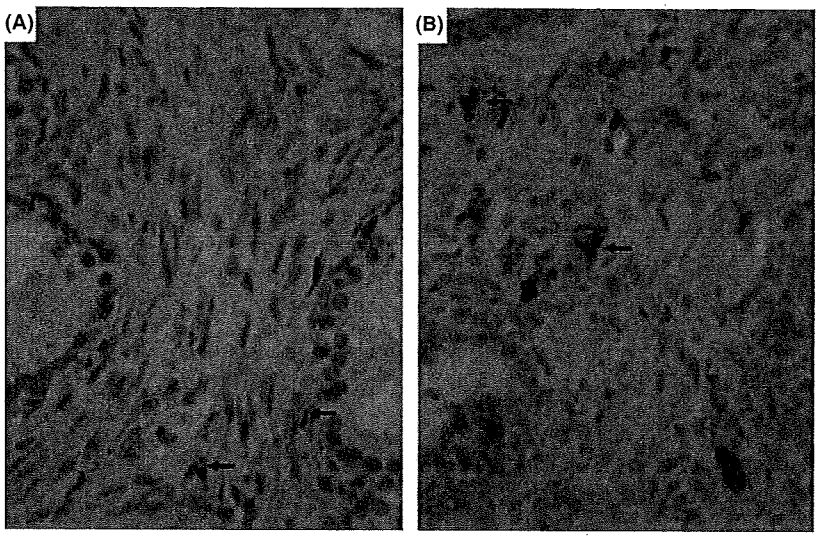

Fig. 1. Representative immunostaining for macrophage scavenger receptor (MSR) cells from men who underwent repeat biopsy of the prostate. Representative cases with low (A) and high (B) MSR counts are shown. Arrowheads indicate MSR-positive cells.

The correlation between TAMs, MSR infiltration by immunohistochemistry, and categorical variables were evaluated using the chi-square test and Fisher's exact probability test. Statistical significance was considered at $P < 0.05$. Logistic regression analysis was carried out to determine significant useful predictors for positive repeat biopsy.

Results

Immunohistochemical findings. Representative immunohistochemical findings are shown in Figure 1. Macrophage scavenger receptor-positive cells were observed among the connective tissue. Prostatic epithelial cells, interstitial cells, or basal cells were not stained with antibody CD204.

Prostate-specific antigen and pathological diagnosis. The PSA value at the first biopsy ranged from 1.7 to 43.12 ng/mL (median, 8.80). The median interval from the first biopsy to the second was 21.6 months (range, 4–84 months). These data are summarized in Table 1. The serum PSA levels at the first biopsy (mean ± SD) did not differ statistically between the patients with final pathological diagnoses of PCa and benign prostate, as shown in Figure 2(A) (11.95 ± 8.39 *versus* 9.19 ± 4.60; $P = 0.075$). In contrast, the PSA level at the repeat biopsy was significantly higher in patients with PCa than in patients with benign prostate (19.65 ± 14.19 *versus* 11.40 ± 8.19; $P = 0.004$; Fig. 2B). No statistical difference in the PSA velocity between PCa and benign prostate was found, as shown in Table 2.

Tumor-associated macrophage count and pathological diagnosis. The TAM count at the first biopsy did not differ between the patients who were diagnosed with PCa and those with benign prostate (16.13 ± 5.85 *versus* 15.70 ± 4.24; $P = 0.364$), as shown in Figure 3.

Macrophage scavenger receptor count and pathological diagnosis. The MSR count at the first biopsy was significantly lower in those patients who were diagnosed with PCa than in

Table 1. Patients' characteristics

	Range	Median
Age at the first biopsy (years old)	51 to 82	69
PSA value at the first biopsy (ng/mL)	1.70 to 43.12	8.80
PSA value at the repeat biopsy (ng/mL)	1.90 to 52.68	10.00
Time from the first to the repeat biopsy (months)	4 to 84	21.6
PSA velocity (ng/mL/year)	−3.77 to 37.50	1.6

PSA, prostate-specific antigen.

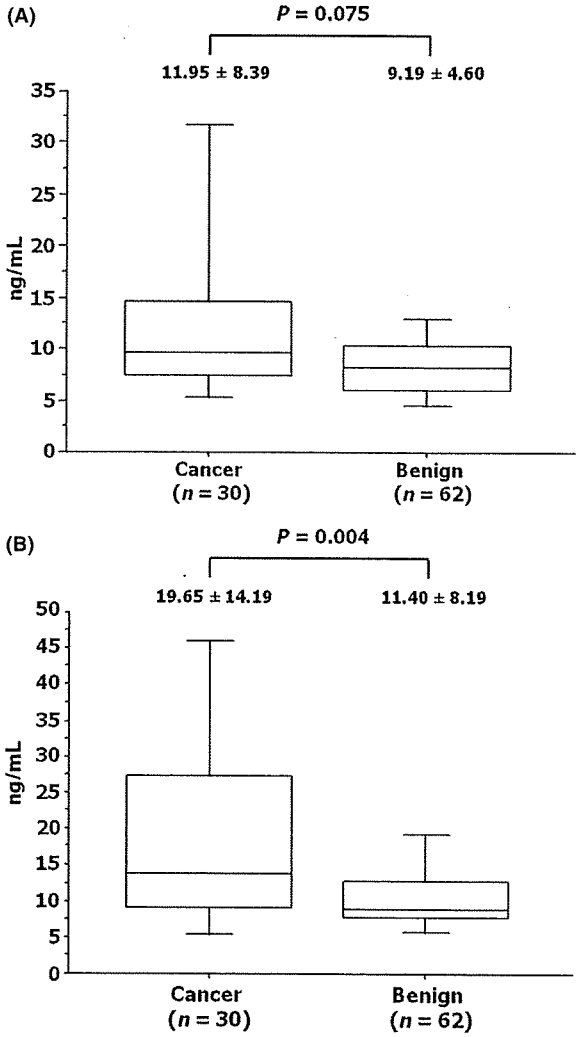

Fig. 2. Association between the final pathological results and the serum prostate-specific antigen level at the first (A) and repeat (B) biopsies of the prostate. Boxed areas represent the 25th and 75th percentiles, and error values; error bars represent the 10th and 90th percentiles.

doi: 10.1111/j.1349-7006.2010.01563.x

Table 2. Association of clinicopathological parameters with biopsy results

	Benign prostate	Prostatic cancer	*P*-value
Age at the repeat biopsy (years)	68.38 ± 6.27	68.98 ± 7.09	0.356
PSA at the first biopsy (ng/mL)	9.19 ± 4.60	11.95 ± 8.39	0.075
PSA at the repeat biopsy (ng/mL)	11.40 ± 8.19	19.65 ± 14.19	0.004
PSA velocity (ng/mL/year)	1.49 ± 4.45	2.72 ± 4.74	0.083
TAM count	15.70 ± 4.24	16.13 ± 5.85	0.364
MSR count	38.70 ± 9.95	27.13 ± 5.28	<0.001

MSR, macrophage scavenger receptor; PSA, prostate-specific antigen; TAM, tumor-associated macrophage.

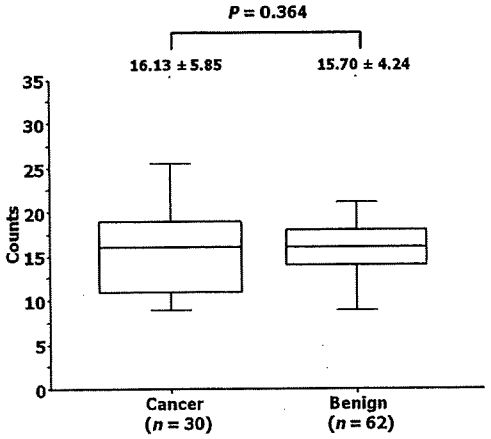

Fig. 3. Association between the tumor-associated macrophage count and pathological results in patients who underwent repeat biopsies of the prostate. Boxed areas represent the 25th and 75th percentiles, and error values; error bars represent the 10th and 90th percentiles.

those with benign prostate (27.13 ± 5.28 *versus* 38.70 ± 9.95; $P < 0.001$) as shown in Figure 4.

Sensitivity and specificity of PSA level, and TAM and MSR counts at first biopsy. The PSA at the first biopsy and the TAM and MSR counts were divided into high and low groups compared to the mean values of 8.80 ng/mL, 16, and 32, respectively. Based on these groupings, sensitivity, specificity, positive predictive value, and negative predictive value were calculated as markers for detecting PCa in the repeat biopsy (Table 3). In Table 3, categories positively associated with cancer are placed upper for PSA, TAM, and MSR. In terms of sensitivity and specificity, the MSR count was superior to the TAM count or PSA level at the first biopsy.

Logistic regression analysis. Among the clinicopathologic parameters analyzed, MSR count was the only useful predictor for positive repeat biopsy (Table 4).

Discussion

With widespread PSA screening, PCa is often detected at an early stage.[2] However, because of the low positive predictive value of PSA, up to 75% of men with gray zone PSA (4–10 ng/mL) cannot escape an unnecessary biopsy.[3] Based on periodic checks, patients with an increasing serum PSA undergo repeat prostate biopsy. Even in those cases, the detection rate of PCa remains between 10% and 35%.[8,21] This means that many people undergo unnecessary biopsies. One of the most serious problems is that indications for repeat biopsy and the timing of the procedure are not clearly defined.[4] Therefore, it is very important to discover a good indicator for a repeat biopsy of the prostate.

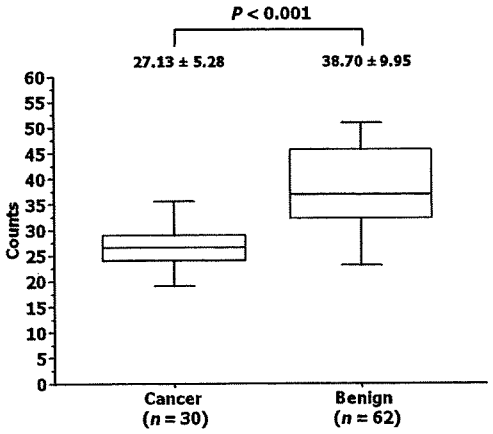

Fig. 4. Association between the macrophage scavenger receptor count and pathological results in patients who underwent repeat biopsies of the prostate. Boxed areas represent the 25th and 75th percentiles, and error values; error bars represent the 10th and 90th percentiles.

Table 3. Sensitivity, specificity, PPV and NPV stratified by PSA, TAM count and MSR count at the first biopsy

Parameter	Benign	Cancer	Sensitivity/ Specificity	PPV*/NPV
High PSA (≥8.8)	27	21	21/30	21/48
Low PSA (<8.8)	35	9	35/62	35/44
High TAM count (≥16)	25	14	14/30	14/39
Low TAM count (<16)	37	16	37/62	37/53
Low MSR count (<32)	18	25	44/62	44/49
High MSR count (≥32)	44	5	25/30	25/43

PSA, prostate-specific antigen; TAM, tumor-associated macrophage; MSR, macrophage scavenger receptor; *PPV, positive predictive value; NPV, negative predictive value.

Table 4. Logistic regression

Parameters	Regression coefficient	*P* value
Age	0.039	0.5583
PSA at the first biopsy	0.0433	0.5182
PSA at the repeat biopsy	0.0531	0.1983
PSA velocity	−0.0639	0.2838
Periods between the first and the repeat biopsy	0.3048	0.1514
TAM count	0.0321	0.6269
MSR count	−0.1972	0.0004

PSA, prostate-specific antigen; TAM, tumor-associated macrophage; MSR, macrophage scavenger receptor.

In our institute, repeat biopsies were carried out based on the doctors' preference and policy according to PSA increase, but not based on definite criteria. Therefore, the interval from the first biopsy to a repeat biopsy was not constant. As shown in Table 2, the PSA levels at the first biopsy of patients with cancer at repeat biopsy were not significantly higher than those of patients without cancer, whereas the PSA levels at the repeat biopsy were higher in patients with cancer than those in patients without cancer. Moreover, PSA velocity tended to be greater in patients with cancer than in patients without cancer. In general, repeat biopsies were likely to be carried out based on the PSA velocity, increased PSA density, low free/total PSA ratio, or the presence of HGPIN.[22–24]

Chronic inflammation of the prostate has been reported to be one of the risk factors for prostate carcinogenesis.[14–17] Several

specific inflammatory cells have been implicated in carcinogenesis or the progression of PCa. The infiltration of TAMs is more prominent in cancer tissue than in normal prostate tissue, and an association between increased infiltration of TAMs and progression of PCa has also been reported.[25,26] Therefore, TAMs might work as cancer-stimulating factors and are usually seen at the tumor–normal tissue interface.[27,28]

Among several species of macrophages, MSR-positive inflammatory cells have been also considered to be M2-polarized and to be involved in the progression of glioma and ovarian epithelial tumor.[29,30] Germ-line mutations of the *MSR1* gene are involved in alterations in host defense immunity as associated with an increased risk of PCa. It has been postulated that defective expression of MSR1, which is associated with macrophage function, could lead to serious inflammatory damage resulting in carcinogenesis.[19–21] Yang *et al.*[18] reported that reduced expression of MSR1 is associated with progression of PCa. Our previous data also showed that decreased infiltration of MSR-positive cells in the prostate biopsy specimens was associated with poor prognosis of the PCa.[31] Moreover, the expression of MSR is inhibited by transforming growth factor-β1 in human monocyte/macrophage cell line THP-1.[32] In humans, an increased level of transforming growth factor-β1 is associated with PCa progression and metastasis.[33] These findings all give us a good reason to accept the results that decreased MSR-positive staining was well correlated with the presence of PCa in the repeat biopsy. Macrophage scavenger receptor-positive cells in the prostate might play protective roles in tumor progression, contrary to other types of malignancies, in spite of no apparent reason.

No reliable or definitive predictor of repeat biopsy outcome is currently available. Other than PSA-related markers, only a few factors have been discussed. Among them, prostate cancer gene 3 mRNA in the urine has been reported to be very useful for patients with elevated serum PSA levels and negative biopsy findings.[9,10] The microvessel density and presence of HGPIN in biopsy specimens have also been reported as useful markers for considering repeat biopsy.[34] In addition, telomerase activity in prostate massage samples and hypermethylation of the glutathione S-transferase gene promoter in the urine after prostate biopsy might be predictive markers, although they have not been evaluated as indicators for a repeat biopsy.[11,12]

Our data needs to be evaluated in a larger sample or pursuing validation study. However, this kind of approach is essential for the discovery of new predicting markers to avoid unnecessary prostate biopsy.

Acknowledgments

This study was supported by Grants-in-Aid from the Japanese Ministry of Education, Culture, Sports, Science and Technology (No. 21592044).

References

1 Jemal A, Siegel R, Ward E *et al.* Cancer statistics, 2008. *CA Cancer J Clin* 2008; **58**: 71–96.
2 Partin AW, Oesterling JE. The clinical usefulness of prostate-specific antigen: update 1994. *J Urol* 1994; **152**: 1358–68.
3 Kirby SR, Christmas TJ, Brawer MK. *Prostate Cancer*. London: Mosby, 2001.
4 Djavan B, Zlotta A, Remzi M *et al.* Optimal predictors of prostate cancer on repeat prostate biopsy: a prospective study of 1,051 men. *J Urol* 2000; **163**: 1144–8.
5 O'Dowd GJ, Miller MC, Orozco R, Veltri RW. Analysis of repeated biopsy results within 1 year after a noncancer diagnosis. *Urology* 2000; **55**: 553–9.
6 Fowler JE Jr, Bigler SA, Miles D, Yalkut DA. Predictors of first repeat biopsy cancer detection with suspected local stage prostate cancer. *J Urol* 2000; **163**: 813–8.
7 Benecchi L, Pieri AM, Melissari M, Potenzoni M, Pastizzaro CD. A novel nomogram to predict the probability of prostate cancer on repeat biopsy. *J Urol* 2008; **180**: 146–9.
8 Shariat SF, Karakiewicz PI, Roehrborn CG, Kattan MW. An updated catalog of prostate cancer predictive tools. *Cancer* 2008; **113**: 3075–99.
9 Marks LS, Fradet Y, Deras IL *et al.* PCA3 molecular urine assay for prostate cancer in men undergoing repeat biopsy. *Urology* 2007; **69**: 532–5.
10 Haese A, de la Taille A, van Poppel H *et al.* Clinical utility of the PCA3 urine assay in European men scheduled for repeat biopsy. *Eur Urol* 2008; **54**: 1081–8.
11 Gonzalgo ML, Pavlovich CP, Lee SM *et al.* Prostate cancer detection by GSTP1 methylation analysis of postbiopsy urine specimens. *Clin Cancer Res* 2003; **9**: 2673–7.
12 Vicentini C, Gravina GL, Angelucci A *et al.* Detection of telomerase activity in prostate massage samples improves differentiating prostate cancer from benign prostatic hyperplasia. *J Cancer Res Clin Oncol* 2004; **130**: 217–21.
13 Coussens LM, Werb Z. Inflammation and cancer. *Nature* 2002; **420**: 860–7.
14 Palapattu GS, Sutcliffe S, Bastian PJ *et al.* Prostate carcinogenesis and inflammation: emerging insights. *Carcinogenesis* 2005; **26**: 1170–81.
15 Wagenlehner FM, Elkahwaji JE, Algaba F *et al.* The role of inflammation and infection in the pathogenesis of prostate carcinoma. *BJU Int* 2007; **100**: 733–7.
16 De Marzo AM, Platz EA, Sutcliffe S *et al.* Inflammation in prostate carcinogenesis. *Nat Rev Cancer* 2007; **7**: 256–69.
17 Sun J, Turner A, Xu J, Gronberg H, Isaacs W. Genetic variability in inflammation pathways and prostate cancer risk. *Urol Oncol* 2007; **25**: 250–9.
18 Yang G, Addai J, Tian WH, Frolov A, Wheeler TM, Thompson TC. Reduced infiltration of class A scavenger receptor positive antigen-presenting cells is associated with prostate cancer progression. *Cancer Res* 2004; **64**: 2076–82.
19 Xu J, Zheng SL, Komiya A *et al.* Germline mutations and sequence variants of the macrophage scavenger receptor 1 gene are associated with prostate cancer risk. *Nat Genet* 2002; **32**: 321–5.
20 Xu J, Zheng SL, Komiya A *et al.* Common sequence variants of the macrophage scavenger receptor 1 gene are associated with prostate cancer risk. *Am J Hum Genet* 2003; **72**: 208–12.
21 Raja J, Ramachandran N, Munneke G, Patel U. Current status of transrectal ultrasound-guided prostate biopsy in the diagnosis of prostate cancer. *Clin Radiol* 2006; **61**: 142–53.
22 Mian BM, Naya Y, Okihara K, Vakar-Lopez F, Troncoso P, Babaian RJ. Predictors of cancer in repeat extended multisite prostate biopsy in men with previous negative extended multisite biopsy. *Urology* 2002; **60**: 836–40.
23 Lopez-Corona E, Ohori M, Scardino PT, Reuter VE, Gonen M, Kattan MW. A nomogram for predicting a positive repeat prostate biopsy in patients with a previous negative biopsy session. *J Urol* 2003; **170**: 1184–8.
24 Puppo P. Repeated negative prostate biopsies with persistently elevated or rising PSA: a modern urologic dilemma. *Eur Urol* 2007; **52**: 639–41.
25 Joseph IB, Isaacs JT. Macrophage role in the anti-prostate cancer response to one class of antiangiogenic agents. *J Natl Cancer Inst* 1998; **90**: 1648–53.
26 Shimura S, Yang G, Ebara S, Wheeler TM, Frolov A, Thompson TC. Reduced infiltration of tumor-associated macrophages in human prostate cancer: association with cancer progression. *Cancer Res* 2000; **60**: 5857–61.
27 Pak CC, Fidler IJ. Molecular mechanisms for activated macrophage recognition of tumor cells. *Semin Cancer Biol* 1991; **2**: 189–95.
28 Sica A, Schioppa T, Mantovani A, Allavena P. Tumour-associated macrophages are a distinct M2 polarised population promoting tumour progression: potential targets of anti-cancer therapy. *Eur J Cancer* 2006; **42**: 717–27.
29 Komohara Y, Ohnishi K, Kuratsu J, Takeya M. Possible involvement of the M2 anti-inflammatory macrophage phenotype in growth of human gliomas. *J Pathol* 2008; **216**: 15–24.
30 Kawamura K, Komohara Y, Takaishi K, Katabuchi H, Takeya M. Detection of M2 macrophages and colony-stimulating factor 1 expression in serous and mucinous ovarian epithelial tumors. *Pathol Int* 2009; **59**: 300–5.
31 Takayama H, Nonomura N, Nishimura K *et al.* Decreased immunostaining for macrophage scavenger receptor is associated with poor prognosis of prostate cancer. *BJU Int* 2009; **103**: 470–4.
32 Nishimura N, Harada-Shiba M, Tajima S *et al.* Acquisition of secretion of transforming growth factor-beta 1 leads to autonomous suppression of scavenger receptor activity in a monocyte-macrophage cell line, THP-1. *J Biol Chem* 1998; **273**: 1562–7.
33 Wikstrom P, Stattin P, Franck-Lissbrant I, Damber JE, Bergh A. Transforming growth factor beta1 is associated with angiogenesis, metastasis, and poor clinical outcome in prostate cancer. *Prostate* 1998; **37**: 19–29.
34 Sinha AA, Quast BJ, Reddy PK *et al.* Microvessel density as a molecular marker for identifying high-grade prostatic intraepithelial neoplasia precursors to prostate cancer. *Exp Mol Pathol* 2004; **77**: 153–9.

doi: 10.1111/j.1349-7006.2010.01563.x

Increased Infiltration of Tumor Associated Macrophages is Associated With Poor Prognosis of Bladder Carcinoma In Situ After Intravesical Bacillus Calmette-Guerin Instillation

Hitoshi Takayama, Kazuo Nishimura, Akira Tsujimura, Yasutomo Nakai, Masashi Nakayama, Katsuyuki Aozasa, Akihiko Okuyama and Norio Nonomura*

From the Departments of Urology and Pathology (KA), Osaka University Graduate School of Medicine, Suita, Japan

Abbreviations and Acronyms

BCG = bacillus Calmette-Guerin

CIS = carcinoma in situ

IL = interleukin

TAM = tumor associated macrophage

TAM-c = TAMs infiltrating among cancer cells

TAM-I = TAMs in lamina propria

Submitted for publication July 15, 2008.

Study received institutional review board approval.

* Correspondence and requests for reprints: Department of Urology, Osaka University Graduate School of Medicine, 2-2 Yamada-oka, Suita, Osaka, Japan 565-0871 (FAX: +81-6-6879-3539; e-mail: nono@uro.med.osaka-u.ac.jp).

See Editorial on page 1532.

Purpose: Tumor associated macrophages can regulate the growth of various cancers positively or negatively. Intravesical bacillus Calmette-Guerin instillation is now gold standard treatment for bladder carcinoma in situ. We investigated the correlation between tumor associated macrophages infiltrating bladder carcinoma in situ and the response to intravesical bacillus Calmette-Guerin therapy.

Materials and Methods: We examined paraffin embedded tissues from 41 patients with bladder carcinoma in situ who received intravesical bacillus Calmette-Guerin therapy. Tumor associated macrophages were immunohistochemically stained by anti-CD68 monoclonal antibody.

Results: The median number of tumor associated macrophages infiltrating among cancer cells and the number in the lamina propria were 4 and 24, respectively. Recurrent carcinoma in situ was found in 4.8% of cases with a lower cancer cell tumor associated macrophage count but in 47.6% of those with a higher cancer cell tumor associated macrophage count (less than 4 vs 4 or greater). Recurrence was found in 31.8% of patients with a lower lamina propria tumor associated macrophage count but in 21.1% of those with a higher lamina propria tumor associated macrophage count (less than 25 vs 25 or greater). The median ratio of tumor associated macrophages among cancer cells vs in the lamina propria was 0.2. Recurrence-free survival was significantly better in patients with a lower cancer cell tumor associated macrophage count ($p = 0.0002$). Those with a lower cancer cell-to-lamina propria tumor associated macrophage ratio had a higher recurrence-free rate ($p < 0.0001$). Multivariate analysis revealed that the cancer cell tumor associated macrophage count and the cancer cell-to-lamina propria tumor associated macrophage ratio can be prognostic factors for bladder carcinoma in situ.

Conclusions: The count of tumor associated macrophages infiltrating the cancer area is useful for predicting the response of bladder carcinoma in situ to intravesical bacillus Calmette-Guerin instillation before treatment initiation.

Key Words: urinary bladder, BCG vaccine, carcinoma in situ, prognosis, macrophages

BLADDER CIS is characterized by areas of flat, anaplastic intraepithelial neoplasms in grossly normal-appearing bladder mucosa.[1] Intravesical BCG instillation has been established as the first choice treatment for bladder CIS.[2,3] Immunotherapy with BCG has resulted in complete tumor regres-

0022-5347/09/1814-1894/0
THE JOURNAL OF UROLOGY®

Vol. 181, 1894-1900, April 2009
Printed in U.S.A.
DOI:10.1016/j.juro.2008.11.090

sion in greater than 70% of treated patients who have bladder CIS.[4,5] Total cystectomy is no longer the generally recommended initial approach. However, muscle invasive disease develops in approximately half of the patients with bladder CIS that does not respond to intravesical BCG instillation, whereas only 10% with initial complete tumor regression after BCG therapy have muscle invasive disease.[6] To date several prognostic markers have been reported. Particularly specific cytokines such as IL-2 and IL-8 in urine have shown prognostic value for tumor recurrence, although the clinical relevance of these cytokines is still debated.[7–10] Therefore, the discovery of markers with which the response of bladder CIS can be predicted before BCG instillation is important to establish appropriate therapeutic modalities.

Tumor cells are surrounded by infiltrating inflammatory cells such as macrophages and mast cells, which communicate via a complex network of intercellular signaling pathways that is mediated by surface adhesion molecules, cytokines and their receptors.[11–14] Leukocytes are known to infiltrate neoplastic tissues. Cells belonging to the monocyte-macrophages lineage are the major components of the leukocyte infiltrate of neoplasms.[11] TAMs originate from circulating blood monocytes. Their recruitment and survival in situ are directed by chemokines and cytokines that interact with tyrosine kinase receptors.[11] TAMs have complex dual functions in their interaction with neoplastic cells (the macrophage balance hypothesis) but strong evidence suggests that they are part of inflammatory circuits that promote tumor progression.[11–14] The presence of TAMs correlates positively with increased vascularity and metastasis, and with decreased relapse-free and overall survival rates in breast cancer and nonsmall cell lung cancer cases.[15,16] Bladder CIS responds to intravesical BCG instillation, suggesting that some infiltrating inflammatory cells may have protective or supportive roles in tumor progression.

However, to our knowledge there has been no study of TAM infiltration in bladder CIS. Thus, we performed immunohistochemical analysis of TAM infiltration in tissues obtained by transurethral resection of the bladder. We investigated whether the prognosis in patients with bladder CIS after BCG instillation could be predicted by TAM infiltration.

MATERIALS AND METHODS

Patients

A total of 41 patients diagnosed with bladder CIS at our hospital from 1995 to 2005 were selected for study. At hospital admission the patients were 47 to 91 years old (median age 70). All patients had positive urine cytology but no visible tumors on endoscopy. A diagnosis of bladder CIS was made by histological examination of specimens obtained by transurethral bladder biopsy. Table 1 lists patient characteristics.

Histological specimens were fixed in 10% neutral buffered formalin and routinely processed for paraffin embedding. Serial 5 μm sections were cut, stained with hematoxylin and reviewed by 1 pathologist. Two weeks after transurethral bladder biopsy the patients started to receive weekly intravesical BCG (80 mg Tokyo 172 or 81 mg Connaught strain) instillations for a total of 6 times. BCG was instilled into the bladder with 40 ml saline and retained for 2 hours. After initial therapy the patients were followed with periodic cystoscopy, ultrasonography, x-ray and urine cytology.

Immunohistochemical Analysis

TAMs were immunohistochemically labeled using CD68 monoclonal antibody (Dako, Glostrup, Denmark). Immunohistochemical study of paraffin sections was done using the LSAB™ method. For systematic counting 6 ocular measuring fields with a real area of 0.06175 mm^2 each were chosen randomly under a microscope at 400× magnification. The number of CD68 positive cells is expressed as the TAM count, including TAM-c, TAM-l and TAMs in the total area.

Statistics

Recurrent bladder CIS was defined as positive cytology. In our study patients who had positive urinary cytology after BCG therapy without exception showed at least 2 consecutive positive urinary cytology results. Time to recurrence was measured from the date of the first intravesical BCG instillation to the first date of positive cytology. Statistical analysis was performed using StatView™. Correlations between immunohistochemically measured TAM infiltration and clinicopathological parameters were evaluated using the chi-square and Fisher exact probability tests. Followup from the date of the start of therapy in survivors was 3.0 to 240.5 months (mean 55.2) (table 1). The recurrence-free survival rate was calculated using the Kaplan-Meier method and differences in survival curves were estimated using the log rank test. Independent prognostic factors were analyzed using a Cox proportional hazards regression model in a stepwise manner with $p < 0.05$ considered statistically significant.

RESULTS

TAM-c and TAM-l in Bladder CIS

CD68 positive cells were observed in all specimens tested. Most CD68 positive cells showed morpholog-

Table 1. *Patient Characteristics*

No. pts	41
No. sex (%):	
M	38 (92.7)
F	3 (7.3)
No. recurrence (%):	
Yes	12 (29.3)
No	29 (70.7)
Median age (range)	70 (47–90)
Median mos followup (range)	25 (3–120)
Median mos recurrence (range)	12 (3–36)

ical features of macrophages. However, TAM-c and TAM-l were detected in 25 of 41 cases with a median count of 3.0 (range 0 to 40) and 24.0 (range 6 to 57), respectively (fig. 1). For further study cases were divided into 2 groups, including 1 group with a higher TAM count than the median value and the other group with a lower TAM count.

TAM Count and Various Clinicopathological Factors

Table 2 lists correlations between the TAM count and various clinicopathological factors. The TAM-c count correlated positively with CIS recurrence ($p = 0.0023$). However, recurrent CIS did not correlate with the TAM-l count or the TAM count in the total area. Patient age and gender did not correlate with TAM counts.

Recurrence-Free Survival

Followup was 3.0 to 120.0 months (mean 52.8). CIS recurrence was found in 4.8% of cases with a lower TAM-c count but in 47.6% with a higher TAM-c count (less than 4 vs 4 or greater). However, recurrent bladder CIS was found in 31.8% of cases with a lower TAM-l count but in 21.1% with a higher TAM-l count (less than 25 vs 25 or greater). Time to recurrence was 3.0 to 37.2 months (mean 13.6). The recurrence-free survival rate was significantly lower in patients with a higher TAM-c count than in patients with a lower TAM-c count ($p = 0.0002$, fig. 2, *A*). However, patients with a higher TAM-l count did not show any significant difference in recurrence-free survival compared to those with a lower TAM-l count (fig. 2, *B*). TAMs in the total area did not correlate with the recurrence-free survival rate (fig. 3, *A*). The TAM-c/TAM-l ratio correlated with CIS recurrence. The recurrence-free survival rate in patients with a higher TAM-c/TAM-l ratio was significantly lower than in those with a lower ratio ($p < 0.0001$, fig. 3, *B*).

Table 2. *Macrophage Count and clinicopathological factors*

Clinicopathological Factors	No. Pts (%)	Mean ± SE Count	p Value
	Count in total area		
Age:			
Younger than 70	21 (51.2)	35.048 ± 16.732	0.2918
70 or Older	20 (48.8)	20.100 ± 16.887	
Sex:			
F	5 (12.2)	25.800 ± 10.232	0.029
M	36 (87.8)	33.028 ± 18.586	
Recurrence:			
Yes	12 (29.3)	30.241 ± 17.679	0.2937
No	29 (70.7)	36.750 ± 18.162	
	Count in lamina propria		
Age:			
Younger than 70	21 (51.2)	27.095 ± 13.057	0.2457
70 or Older	20 (48.8)	22.550 ± 11.546	
Sex:			
F	5 (12.2)	24.600 ± 11.760	0.9581
M	36 (87.8)	24.917 ± 12.650	
Recurrence:			
Yes	12 (29.3)	22.750 ± 8.357	0.868
No	29 (70.3)	25.759 ± 13.770	
	Count in Ca area		
Age:			
Younger than 70	21 (51.2)	7.952 ± 8.133	0.6408
70 or Older	20 (48.8)	6.550 ± 10.836	
Sex:			
F	5 (12.2)	1.200 ± 1.643	0.1271
M	36 (87.8)	8.111 ± 9.789	
Recurrence:			
Yes	12 (29.3)	14.00 ± 11.176	0.0023
No	29 (70.3)	4.483 ± 7.150	

Multivariate Survival Analysis

Cox multivariate analysis indicated that the TAM-c count and the TAM-c/TAM-l ratio were independent prognostic factors for CIS ($p = 0.0012$ and 0.0032, respectively, table 3).

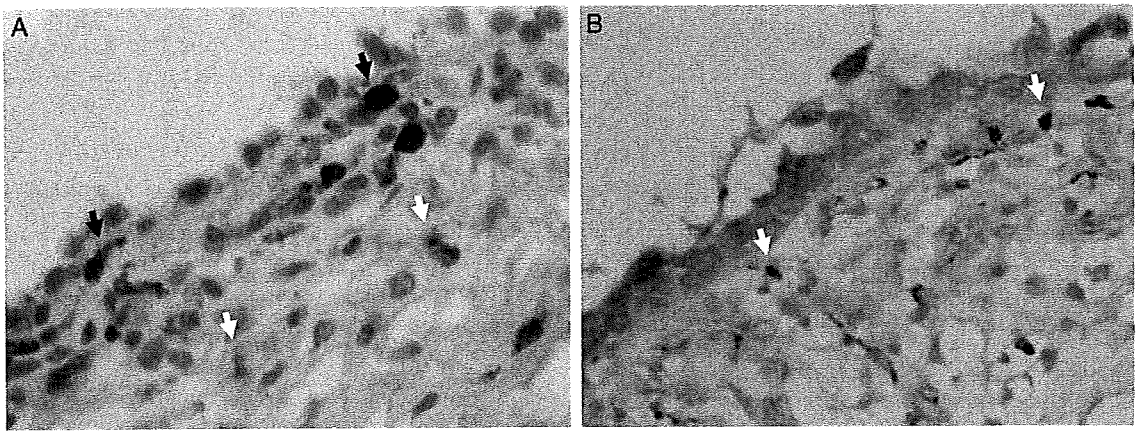

Figure 1. TAM immunostaining of bladder CIS using monoclonal antibody. *A*, strong staining. Black arrows indicate TAMs in cancer area. *B*, faint staining. White arrows indicate TAMs in lamina propria. Reduced from ×400.

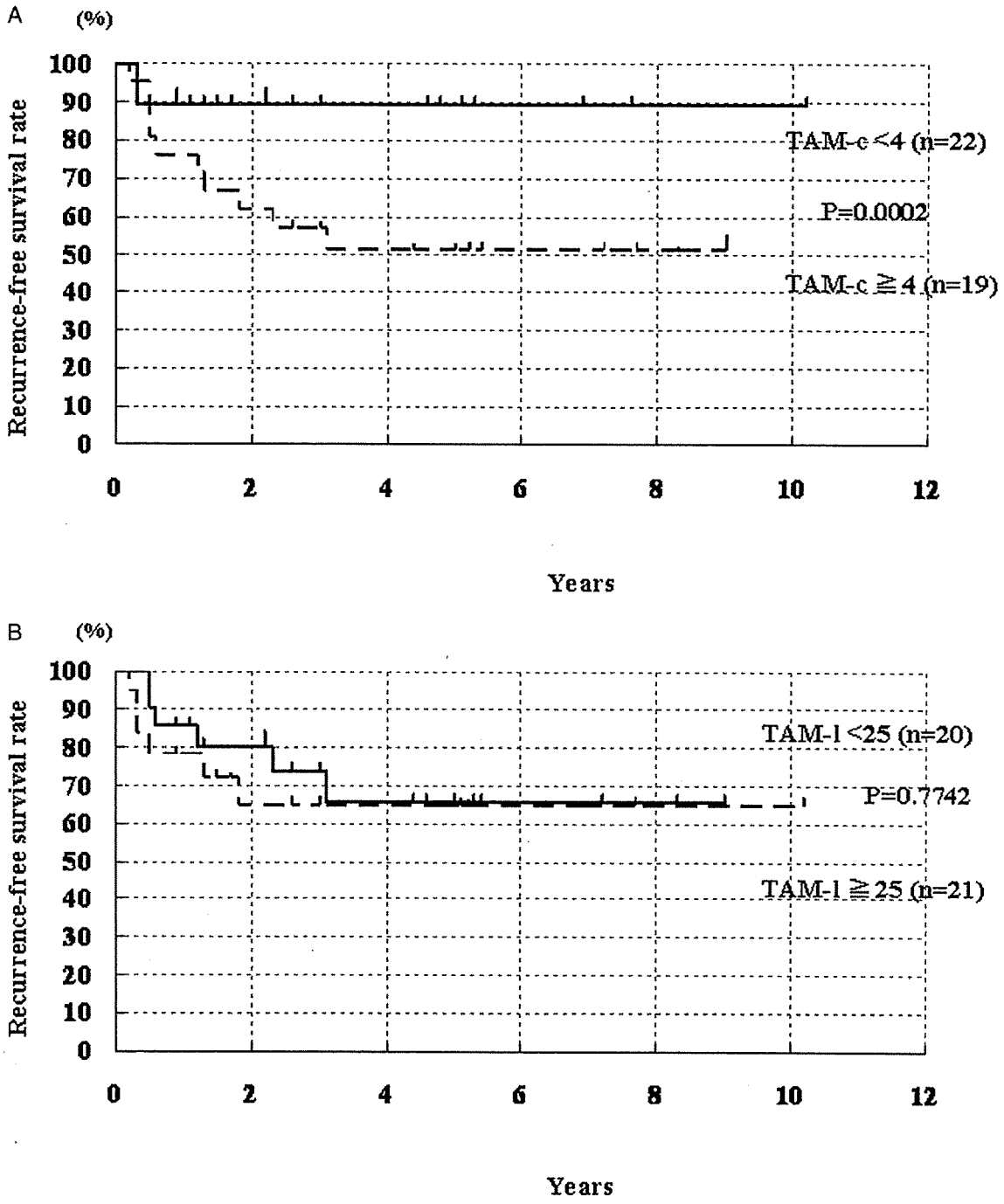

Figure 2. Recurrence-free survival in patients with bladder CIS and high or low TAM count. *A*, TAM-c (significantly different, p = 0.0002). *B*, TAM-l.

DISCUSSION

Bladder CIS represents a distinct form of urothelial cancer. Urothelial CIS is characterized by flat, disordered proliferation of urothelial cells with marked cytological abnormalities. Most cases develop in men older than 50 years who complain of cystitis-like symptoms. In fact submucosal tissue is accompanied by the infiltration of many inflammatory cells. These inflammatory cells contain nonspecific inflammatory cells as well as cancer specific inflammatory cells such as macrophages and mast cells. These inflammatory cells communicate via a complex network of intercellular signaling pathways that is mediated by cell surface adhesion molecules, cytokines and their receptors. Some of these cancer associated inflammatory cells are macrophages known as TAMs.[11–14]